Journal of Aerosol Science 183 (2025) 106471

Contents lists available at ScienceDirect

Journal of Aerosol Science

journal homepage: www.elsevier.com/locate/jaerosci

Subject-specific multi-scale modeling of the fate of inhaled aerosols

A.P. Kuprat [a,*], Y. Feng [b], R.A. Corley [c], C. Darquenne [d]

[a] Pacific Northwest National Laboratory, Richland, WA, USA
[b] School of Chemical Engineering, Oklahoma State University, Stillwater, OK, USA
[c] Greek Creek Toxicokinetics Consulting, LLC, Boise, ID, USA
[d] Department of Medicine, University of California, San Diego, CA, USA

ARTICLE INFO

Keywords:
Aerosol dosimetry
Subject-specific modeling
Multi-scale modeling
Computational fluid particle dynamics (CFPD)
Physiologically-based pharmacokinetics (PBPK)
Host cell dynamics (HCD)

ABSTRACT

Determining the fate of inhaled aerosols in the respiratory system is essential in assessing the potential toxicity of inhaled airborne materials, responses to airborne pathogens, or in improving inhaled drug delivery. The availability of high-resolution clinical lung imaging and advances in the reconstruction of lung airways from CT images have led to the development of subject-specific in-silico 3D models of aerosol dosimetry, often referred to as computational fluid-particle-dynamics (CFPD) models. As CFPD models require extensive computing resources, they are typically confined to the upper and large airways. These models can be combined with lower-dimensional models to form multiscale models that predict the transport and deposition of inhaled aerosols in the entire respiratory tract. Understanding where aerosols deposit is only the first of potentially several key events necessary to predict an outcome, being a detrimental health effect or a therapeutic response. To that end, multiscale approaches that combine CFPD with physiologically-based pharmacokinetics (PBPK) models have been developed to evaluate the absorption, distribution, metabolism, and excretion (ADME) of toxic or medicinal chemicals in one or more compartments of the human body. CFPD models can also be combined with host cell dynamics (HCD) models to assess regional immune system responses. This paper reviews the state of the art of these different multiscale approaches and discusses the potential role of personalized or subject-specific modeling in respiratory health.

1. Introduction

Determining the fate of inhaled aerosols in the respiratory system has been the focus of intense research in the last few decades as such knowledge is essential in assessing the potential toxicity of inhaled airborne materials, responses to airborne pathogens and viruses, or in improving the delivery of inhaled drugs. There have been a multitude of *in silico*, *in vitro, ex vivo* and *in vivo* approaches used to address this complex problem. The present literature review focuses on multiscale *in silico* models of aerosol dosimetry. Multiscale models use mathematics and computational approaches to quantitatively represent and simulate a system at more than one scale while functionally linking the mathematical models across these scales. For aerosol dosimetry applications, several types of multiscale models have been developed. In this review, we first discuss the evolution of predictive models of aerosol deposition and the

* Corresponding author. Pacific Northwest National Laboratory, P.O. Box 999, MSIN J4-18, Richland, WA, 99352, USA.
E-mail address: Andrew.Kuprat@pnnl.gov (A.P. Kuprat).

https://doi.org/10.1016/j.jaerosci.2024.106471
Received 13 May 2024; Received in revised form 17 September 2024; Accepted 18 September 2024
Available online 19 September 2024

rationale behind the need for multiscale approaches, including subject-specific model advancements as they contribute to the overall movement towards digital twin technologies. We further included multiscale models that link aerosol deposition to physiologically-based pharmacokinetic (PBPK) models that improve local or systemic tissue dose predictions and finally, on models linking aerosol deposition to pharmacodynamic, biological response models such as the Host Cell Dynamics (HCD) models that predict immune responses post deposition and in particular, those following deposition of viral particles.

2. Multiscale models of aerosol transport and deposition

2.1. Why multiscale modeling?

In silico predictions of aerosol deposition in the respiratory system of humans and laboratory animals require the modeling practitioner to incorporate, at a minimum, a basic understanding of species-specific anatomy and physiology along with physical/chemical properties of the aerosol that are critical to predicting the fate and transport over the full system. Historically, aerosol dosimetry models have fallen into two main categories: semi-empirical or one-dimensional (1D) mechanistic models. As previously reviewed by Longest (Longest et al., 2019), semi-empirical models were generally based upon fitting empirical measurement data to a series of parameters used in analytical equations. Such models can provide accurate predictions of particle deposition in airway regions as long as the aerosol properties and exposures are consistent with empirical data used to define the model.

As an alternative approach to semi-empirical models, 1D mechanistic models of the respiratory system represent aerosol fate and transport in airways using equations based upon biological properties such as airway size (e.g. length, diameter, etc.), ventilation profile (e.g. nasal vs. oral, minute volume, frequency, functional residual capacity, total lung capacity, etc.) and physical mechanisms of aerosol transport (e.g. convective flow, diffusion, particle interactions, hygroscopicity, etc.) and deposition (e.g. sedimentation, impaction, diffusion) (Darquenne & Paiva, 1994; Taulbee & Yu, 1975). This approach is therefore based more upon first principles rather than upon fitting of parameters to specific empirical data sets. As such, 1D mechanistic models are useful for predicting aerosol deposition for a variety of exposure conditions once the biological and aerosol properties are specified.

For decades, ICRP (ICRP, 1994, 2015) or NCRP (NCRP, 1997) models for human exposures to radionuclide particles were considered state of the art for aerosol dosimetry models. The ICRP is a semi-empirical model while the NCRP model is a hybrid, semi-empirical (extrathoracic region) and 1D mechanistic model (lung), commensurate with the model structure, assumptions, and data available (e.g. gamma scintigraphy). To address additional types of environmental aerosol exposures, the multiple path particle dosimetry (MPPD) model, which includes many aspects of the ICRP and NCRP models, is probably the best known and most widely utilized example of a hybrid semi-empirical (head region) and 1D mechanistic model (tracheobronchial and pulmonary regions) that also covers the entire respiratory system using additional sources of anatomic data. Its rise in popularity is largely due to its ease of use and public availability (https://www.ara.com/mppd/), the incorporation of multiple laboratory animal and human models, the multitude of aerosol types and exposure conditions that can be simulated, and the inclusion of particle clearance processes such as those now found in the ICRP (2015) model, to name a few. Because of its broad applicability and multiple species, MPPD is currently being updated for use by the U.S. EPA to replace its outdated RDDR model (EPA, 2021).

As useful and computationally easy as semi-empirical and 1D mechanistic models are as first approximations of aerosol deposition, neither approach incorporates realistic 3D airway anatomic features that vary considerably between species and individuals. As a result, these models cannot predict site-specific deposition patterns of aerosols within each airway region featured in semi-empirical and 1D mechanistic models. This is especially important for the extrathoracic airway region (nose/mouth through throat) where 3D anatomy and physiology are highly complex and diverse across species and individuals which together influence local airflows, aerosol fate and its ability to penetrate into the deep lung. With the advent of high-resolution medical imaging systems and the rapid advances in computational capabilities over the past few decades, 3D computational fluid dynamics (CFD) approaches are increasingly being developed and applied to study gas/vapor flow and aerosol deposition at high resolution in respiratory airways of animals and humans (from the nose or mouth through several generations of the tracheobronchial region). CFD-based models incorporate partial differential equations that govern mass, momentum, and energy transport across a 3D domain (computational volumetric mesh) along with well-established governing equations covering mechanisms of material transport and deposition that are solved using increasingly more efficient matrix solution algorithms.

This mechanistic, spatial modeling approach was initially developed and continues to be refined for use in many physical science applications, including aerospace, automotive, HVAC (heating, ventilation, air conditioning) systems, heat transfer and thermal management, and environmental engineering. Biological applications in cardiovascular, ocular, and respiratory research have since benefited from the infrastructure initially developed by the physical and engineering sciences. For the respiratory system, 3D CFD modeling applications have undergone their own renaissance over the past 30 years in understanding hazards associated with airborne chemical or biological exposures as well as the design and development of inhaled pharmaceutical drug delivery systems.

Numerous reviews have been published on the application of semi-empirical, 1D mechanistic, and CFD modeling approaches in general (Koullapis, Ollson, Kassinos, & Sznitman, 2019; Longest et al., 2019; Longest & Holbrook, 2012; Oakes, 2024; Rostami, 2009). These reviews, as well as original publications, have clearly shown that the major strength of 3D CFD-based approaches to aerosol modeling (sometimes referred to as computational fluid-particle-dynamics or CFPD modeling) is their ability to utilize actual measured breathing profiles and realistic airway geometry, along with aerosol properties in their predictions of local airway transport and high-resolution, site-specific deposition of aerosols under a variety of exposure conditions in animals and humans. The key weakness of current CFPD models is associated with the high computational demands that are placed upon simulating aerosol transport and deposition in 3D geometries that typically extend from the nose or mouth through ~5–10 generations of the bronchial airways of

animals and humans. Even when accurate 3D airway geometries are available to extend the models to the deep lung, for example by CT imaging lung casts from rats or cryomicrotome imaging lungs from mice (Bauer, Krueger, Lamm, Glenny, & Beichel, 2020; Beichel, Glenny, Bauer, Krueger, & Lamm, 2019; Einstein et al., 2008), the computational limitations for this level of 3D complexity have yet to be overcome and such data have mostly been incorporated into 1D models such as MPPD. For humans, accurate 3D geometry data of the deep lung and alveolar regions that could be utilized in CFD models are also only available from postmortem samples due to radiation dose limitations (CT) in live subjects or lower resolution by alternative approaches (e.g. MRI). As with animal models, extending CFD models to the deep lung, including the alveolar structures, poses considerable computational challenges although newer approaches are being developed to explicitly address this region (Koullapis, Hofemeier, Sznitman, & Kassinos, 2018; Koullapis, Stylianou, Sznitman, Olsson, & Kassinos, 2020). This means that the current state of the art for stand-alone CFPD simulations in the respiratory system has largely been restricted to specific airways, mostly the upper conducting airways along with several generations of the lung with boundary conditions appropriate for local airflow and material transport for bronchial outlets at the end of the CFPD domain. This limitation forces us to either assume equal boundary conditions across all airway outlets that ignore the influence of the regional transmural pressures in the deep lungs that produce heterogeneities in airflow (and particle transport) between lobar regions and across the whole lung or assume boundary conditions across airway outlets based upon experimental regional pressure or airflow data if available. Furthermore, current CFPD simulations cannot address the fate of aerosols that leave the bronchial airway outlets during inhalation, the fraction that deposits in the deeper reaches of the lung, and the remaining fraction capable of returning to the 3D domain during exhalation for eventual deposition or exhalation. These limitations have been the major driving forces for the advent of single path, whole-lung, and multiscale models of the respiratory system that are the subject of this review. The goal of such models is to take advantage of the strengths of CFPD models with the incorporation of realistic airway anatomy for the upper conducting airways for site-specific deposition with simplifications of 3D anatomy of the deep lung or 1D models for the whole-lung where regional airway generation or segment is sufficient resolution for dosimetry assessments to fit within current computational capabilities.

2.2. *Why subject-specific modeling?*

As discussed above, *in silico* models have played a significant role in gaining a better understanding of the fate of inhaled aerosols in the human lung and in studying the effect of anatomy, breathing patterns, and aerosol characteristics on the extent and regional patterns of deposited particles. Thanks to the availability of high-resolution clinical lung imaging and the development of semi-automated reconstruction of lung airways from MR or CT images, there has been a major focus in the last decade on developing subject-specific *in silico* models of aerosol dosimetry. These models offer a unique tool to better mimic the effect of airborne particulate exposure on an individual basis or to personalize inhaled therapy recommendations. Subject-specific models are important as large intrasubject variability in aerosol deposition exists, not only in overall deposition but also in terms of regional deposition. The extrathoracic airways (i.e., nose and mouth) are a major source of variability in aerosol deposition. This is not only the result of a large intersubject variability in upper airway size and shape but also because of a large intrasubject variability if care is not taken into standardizing imaging protocol. Indeed, the breathing mode (oral, nasal, oro-nasal), the position of the tongue and mandibles and the distensibility of the upper airway all affect upper airway volume and shape (Darquenne et al., 2018; Nikander, von Hollen, & Larhrib, 2017; Schwab, Gefter, Hoffman, Gupta, & Pack, 1993). The variability in upper airway deposition has been demonstrated in multiple *in vivo* (Bennett & Zeman, 2005; Chan & Lippmann, 1980; Emmett, Aitken, & Hannan, 1982; Foord, Black, & Walsh, 1978; Heyder & Rudolf, 1975; Hounam, Black, & Walsh, 1970; Lippmann, 1976; Rasmussen, Swift, Hilberg, & Pedersen, 1990; Stahlhofen, Gebhart & Heyder, 1980, 1981; Stahlhofen, Gebhart, Heyder, & Scheuch, 1983), *in vitro* (Cheng, Zhou, & Chen, 1999; Garcia, Tewksbury, Wong, & Kimbell, 2009; Golshahi, Noga, Vehring, & Finlay, 2013; Grgic, Finlay, Burnell, & Heenan, 2004) and *in silico* studies (Borojeni et al., 2023; Feng et al., 2018a; G. J. Garcia, Schroeter, et al., 2009; Longest & Holbrook, 2012). While the filtering effect of the upper airway serves as a protective mechanism to prevent inhaled particulate toxicants from reaching the lungs, it also presents a barrier to the delivery of inhaled drug particles. For example, Borojeni and colleagues (Borojeni et al., 2023) showed that, for an optimal size distribution of 1–5 μm for pharmaceutical aerosols, over 75% of the inhaled aerosol was delivered to the intrathoracic lungs in most of the 11 subjects they studied for resting tidal breathing conditions but only in about half the subjects when inhaled flow was increased to match that reached when using a dry powder inhaler.

Beyond the extrathoracic airways, there are known differences in lung volumes, airway size, and breathing patterns based on age, sex, and body size (Christou et al., 2021; Dominelli et al., 2018). These and other factors affecting the distribution of inspired air within the intrathoracic lungs (such as lung compliance and disease state) also strongly affect aerosol transport and, ultimately, the spatial distribution of deposited particles. Thus, knowledge of subject-specific ventilation distribution is essential for accurate predictions of regional deposition patterns. Early models typically assumed that regional ventilation is proportional to regional subtended lung volume (Asgharian, Hofmann, & Bergman, 2001; Yeh & Schum, 1980). However, even in healthy subjects, non-uniform ventilation exists between the upper and lower lung lobes, with the lower lobes receiving a larger fraction of inspired air (De Backer et al., 2010; Yamada et al., 2020), affecting regional deposition (Kuprat et al., 2023). The presence of lung disease and the accompanying heterogeneous pathophysiology bring additional heterogeneity in ventilation distribution, further complicating accurate modeling of flow and aerosol deposition. It is thus not surprising that only a few CFPD studies have focused on lung diseases (Darquenne, Corcoran, Lavorini, Sorano, & Usmani; Poorbahrami, Mummy, Fain, & Oakes, 2019; Sadafi, Monshi Tousi, De Backer, & De Backer, 2024; Vinchurkar et al., 2012) and even less, if any, have provided airway-specific deposition information in the small airways (diameter < 2 mm) that are known to be a major site of inflammation and remodeling in diseases such as asthma and COPD. This complexity could be partially addressed using multiscale strategies that couple 3D CFPD models of the upper airway and large conducting airways with lower-dimensional models that incorporate distal lung mechanics based on subject-specific clinical tests such as spirometry,

plethysmography, imaging, etc. Such models could then become an effective tool to explore and understand the connection between disease, diagnosis, and inhaled therapy outcomes on an individual basis. The degree of subject-specificity should, however, be adapted to the intended application. For example, risk assessment studies typically focus on population characteristics. In this instance, population-specific airway models (Kannan et al., 2020) should be considered rather than individual-based models. Alternatively, in the emerging field of digital twins in medicine, individual-based aerosol dosimetry models could play a major role, allowing for dynamic simulations of potential inhaled therapy treatment strategy, monitoring and prediction of health trajectory.

2.3. Current models

2.3.1. CFPD modeling

Simulating the transport and deposition of aerosols in the lung using CFPD requires both airflow and particle transport to be tracked. The airflow model solves the incompressible Navier-Stokes equations:

$$\nabla \bullet \boldsymbol{u} = 0 \tag{1a}$$

$$\rho\left(\frac{\partial \boldsymbol{u}}{\partial t} + (\boldsymbol{u} \bullet \nabla)\boldsymbol{u}\right) = -\nabla \mathrm{p} + \mu\Delta\boldsymbol{u} + \rho\boldsymbol{g} \tag{1b}$$

where $\boldsymbol{u}$ is the velocity vector, ρ and $\boldsymbol{\mu}$ are the density and dynamic viscosity of the fluid (i.e., air), p is pressure and t is time. These equations suffice for laminar flow. However, the upper airways can exhibit transitional or turbulent flow at Reynolds numbers ~2000 or above depending upon the geometry and breathing conditions. In this situation, the computational requirements for direct numerical simulation (DNS) of turbulence are exceedingly high due to the small length scale of the turbulent flow. However, a modification of (Eq. (1)) can be utilized to create an approximation of the true solution when turbulence is present. The Reynolds-averaged Navier-Stokes (RANS) equations are obtained by positing the flow velocity $\boldsymbol{u}$ in the Navier-Stokes equations is the sum of a slowly varying component $\boldsymbol{U}$ and a rapidly fluctuating component $\boldsymbol{u}'$. Inserting $\boldsymbol{u} = \boldsymbol{U} + \boldsymbol{u}'$ into (Eq (1)) and then averaging over a short time scale results in an equation for the slowly varying component $\boldsymbol{U}$ of flow which is identical to (Eq. (1)), with $\boldsymbol{u}$ replaced by $\boldsymbol{U}$, but which has an additional term $-\frac{\partial}{\partial x_j}\tau_{ij} = -\frac{\partial}{\partial x_j}\rho\overline{u_i'u_j'}$ added to the right hand side of (Eq. (1b)). τ_{ij} is known as the Reynolds stress and $\overline{u_i'u_j'}$ represents the time-averaged value of $u_i'u_j'$. In principle, τ_{ij} has six independent components and indeed does exhibit anisotropy near walls. One approach is thus solving for the components which is done in the Reynolds Stress Model (RSM). However, if it is assumed that the Reynolds stress arises from an isotropic turbulent viscosity μ_T, then evaluation of the Reynolds stress becomes considerably less computationally expensive. Popular RANS models making this assumption are the two-equation k-ε and k-ω family of models. The most popular RANS model in use for modeling turbulence in respiratory geometries is the SST k-ω model where τ_{ij} can be evaluated by solving two additional equations (Eq. (2)).

$$\frac{\partial(\rho k)}{\partial t} + \frac{\partial(\rho U_i k)}{\partial x_i} = \widetilde{P_k} - \beta^*\rho k\omega + \frac{\partial}{\partial x_i}\left[(\mu + \rho\sigma_k\nu_T)\frac{\partial k}{\partial x_i}\right] \tag{2a}$$

$$\frac{\partial(\rho\omega)}{\partial t} + \frac{\partial(\rho U_i \omega)}{\partial x_i} = \alpha\rho S^2 - \beta\rho\omega^2 + \frac{\partial}{\partial x_i}\left[(\mu + \rho\sigma_\omega\nu_T)\frac{\partial\omega}{\partial x_i}\right] + 2(1 - F_1)\rho\sigma_{\omega 2}\frac{1}{\omega}\frac{\partial k}{\partial x_i}\frac{\partial\omega}{\partial x_i} \tag{2b}$$

Solution of these additional equations frequently does not require significant extra computational resources compared to laminar flow computations. Here k is turbulence kinetic energy (equal to half the trace of the Reynolds stress) and ω is specific turbulence dissipation rate. Details of the model with suggested values for the various parameters can be found in (Menter, 1993, 1994; Menter, Kuntz, & Langtry, 2003). Recommendations for obtaining accurate deposition results using two-equation RANS turbulence models can be found in (Bass & Worth Longest, 2018).

Alternatively, large eddy simulation (LES) can be employed which involves spatial averaging (rather than time-averaging) of the Navier-Stokes equations and this can be more accurate than RANS (Salim, Ong, & Cheah, 2011). However, LES requires 100-fold more computational resources than RANS models (Zhang & Kleinstreuer, 2011) and is thus impractical for most respiratory geometries.

There are several commercial CFD solvers that can be used for the solution of Eqs. (1) and (2) for respiratory geometries with Fluent (ANSYS, 2024b) being the most popular along with Star-CCM+ (Siemens Digital IndustriesSoftware, 2022). For commercial use, these solvers are relatively expensive, although these software packages are usually available at a discount at educational institutions. The most common open-source software for solving equations (1) and (2) is OpenFOAM (https://www.openfoam.com/). Although the software itself is free, the user is somewhat on their own when using the software, although message boards (http://www.cfd-online.com) exist to answer questions and for-fee consultation is also available. One sticking point with the use of open-source software is that production of the 3D computational mesh (consisting of general polyhedra, hexahedra, tetrahedra, and triangular prisms) suitable for laminar or turbulent flow simulation in the complex 3D respiratory domain is usually only of sufficient quality when commercial meshing products are employed. Thus, it is common to generate a 3D mesh with a commercial solver and then to actually employ an open-source solver to compute on the mesh.

For spherical particles of size order 1 μm or larger, the aerosol phase is most commonly modeled using the Lagrangian method in the 3D domain (Eq. (3)).

$$\frac{d\boldsymbol{u}_p}{dt} = \frac{3}{4}\frac{C_D|\boldsymbol{u}-\boldsymbol{u}_p|\rho}{C_C d_p \rho_p}(\boldsymbol{u}-\boldsymbol{u}_p) + \frac{\boldsymbol{g}(\rho_p-\rho)}{\rho_p} \tag{3}$$

Here, $\boldsymbol{u}_p$, d_p, ρ_p are particle velocity, diameter, and density, C_D is drag coefficient, C_C is Cunningham correction factor, and $\boldsymbol{g}$ is the gravity acceleration vector. The first term on the right-hand side arises from the force of particle drag, while the second term arises from the force of gravity, less the effect of buoyancy. Eq. (3) is used for tracking individual computational 'parcels' in the 3D domain. A computational parcel represents potentially a variable number of actual aerosol particles. If absolute particle concentration drops, such as number of particles injected into 3D domain upon exhalation versus number of particles injected into 3D domain upon inhalation, parcels may be redefined to represent a lower number of actual particles. This increases the number of parcels injected, so that there is still a sufficient number of parcels to give good spatial distribution statistics. (Oakes, Shadden, Grandmont, & Vignon-Clementel, 2017). In the literature, it is common to simply refer to computational parcels as 'particles'.

Typically for micron scale particles, the number density of inhaled particles is low enough that it is acceptable to treat the particles as not influencing the momentum of the airflow and not colliding with or influencing the trajectory of other particles. In dense aerosols (particle volume fraction $> 10^{-6}$) the particles must be treated as influencing the flow and, in extremely dense aerosols, particle interactions with other particles must be considered (Kuerten, 2016). For particles smaller than 1 μm, a Gaussian noise term is added to the right-hand side of the Lagrangian particle evolution equation (Eq. (3)), representing the effect of Brownian motion (due to thermal fluctuations) which is significant for smaller particles (Asgharian & Anjilvel, 1994; Longest & Xi, 2007). Additionally, particles from metered dose inhalers (MDI) and dry powder inhalers (DPI) can possess relatively large ionic charges which then feel an attractive electrostatic force to nearby lung tissue which acts as a polarized dielectric (Bessler & Sznitman, 2024). Modeling this effect requires addition of another term to the right-hand side of Eq (3) and simulations have shown significant particle deposition increase, especially for sub-micron particles (Koullapis, Kassinos, Bivolarova, & Melikov, 2016). Other forces that influence particle motion (i.e., Saffman, Basset, Pressure Gradient, Faxen, Magnus) have been shown to be small compared to the drag force and can usually be neglected for spherical particles (Kleinstreuer & Feng, 2013). If particle mass changes due to hygroscopic growth, evaporation, or condensation, Eq. (3) can be solved, provided there is a relationship known for determining evolution of particle diameter d_p. (See for example (Feng, Kleinstreuer, Castro, & Rostami, 2016; Longest & Hindle, 2011)).

Velocity fluctuations due to turbulence on very small timescales are effectively averaged out by the methodology of the RANS model of turbulence. However, particles experience the fluctuations and become diffused, similar to the effect of Brownian diffusion. As suggested by Ahmadi (He & Ahmadi, 1999; Li & Ahmadi, 1992; Mofakham & Ahmadi, 2020; Tian & Ahmadi, 2007), adding a Gaussian velocity perturbation to **u** on the right-hand side of Eq. (3) can correctly account for the diffusive effect of very rapid velocity fluctuations in the Lagrangian simulation of particle motion. However as acknowledged in Fluent documentation (ANSYS, 2024a), utilization of the 'turbulent dispersion of particles (stochastic tracking)' feature in Fluent "is known to give poor prediction of wall impaction rate of particles with a diameter less than a few microns due to turbulence". As noted in (Mofakham & Ahmadi, 2020), the Fluent algorithm as implemented leads to overestimation of particle deposition due to failure to account for the quadratic reduction in the normal velocity fluctuations in the viscous sublayer adjacent to the wall. Since solely enabling Brownian diffusion more correctly represents particle diffusion in the viscous sublayer and hence deposition in the case of nanoparticles, it is recommended not to enable the "stochastic tracking" feature in Fluent but rely upon the Brownian diffusion feature instead. However (Mofakham & Ahmadi, 2020) utilize UDF (user-defined functions) that can be used in Fluent (and which in principle can be converted for use in other CFPD solvers) which correctly treat turbulent diffusion in the boundary layer. Since it is shown in (Li & Ahmadi, 1992) that outside the viscous sublayer, turbulent diffusion dominates Brownian diffusion even for nanoparticles, one would hope that at some point the Fluent code will treat stochastic tracking properly, as turbulent diffusion has an important effect on particle motion over the whole size range when turbulent or transitional flow is present.

Alternatively, for nanoparticles of size <100 nm, particles can be represented as a continuum particle concentration field that is advected and diffused by the airflow and where particle inertia is neglected. This is known as the Eulerian representation of particles (Longest & Xi, 2007). This Eulerian representation is also commonly used in the computation of toxic or medicinal vapor advection and diffusion in the lung. An extremely challenging case is typical in e-cigarette vapor respiration. Here, the chemical emissions from the e-cig device are inhaled as a combination of vapor and particles. In this case, it may be necessary to model the evaporation of chemicals in the entrained particles into vapor form, as well as the hygroscopic growth of the particles as they proceed down the respiratory tract (Feng et al., 2016).

2.3.2. Multiscale models

As mentioned above, CFPD models typically focus on the upper and large conducting airways. To allow predictions to be made for the entire lung, multiscale strategies have been developed that couple these 3D CFPD models with lower-dimensional models that incorporate the distal lung. Airflow in the lower-dimensional models can be determined in various ways. In a true one-dimensional airflow model, the Navier-Stokes equations are integrated over airway cross-sections to produce a one-dimensional partial differential equation ("1D-NS") (Peiró & Veneziani, 2009). More commonly, the airways are treated using RLC (resistance-inertance-compliance) models that are 0-dimensional (0D) (i.e., ordinary differential equations (ODEs)) (Ismail, Comerford, & Wall, 2013) and which are sometimes still referred to as "1-dimensional" models. The most basic model of airflow (for which there is good evidence at least for healthy subjects) has the airflow in an airway generation being proportional to the volume distal to that generation (Anjilvel & Asgharian, 1995). For the representation of gases and aerosols in lower-dimensional models, the Eulerian representation must be used where a continuum field represents gas or particle concentration and is resolved by a one-dimensional partial differential equation

(PDE), which takes into account advection, diffusion, gravitational sedimentation, and impaction into bifurcations.

The geometry of the lower-dimensional human airway models was originally represented as a regular bifurcating model with ~24 generations starting at the trachea and ending with $2^{23}\approx 8.4$ million terminal airways (alveolar sacs). The first 16 generations comprise the conducting airways, while the last 8 generations are the alveolated respiratory airways (Weibel, 1963). The regular bifurcating model of course deviates from the true human respiratory geometry, as asymmetry exists as the airways proceed into the 5 lobes: not only the airway bifurcation angles but also the number of bifurcations in a given path from the trachea to an alveolar sac vary considerably (Haefeli-Bleuer & Weibel, 1988; Horsfield, Dart, Olson, Filley, & Cumming, 1971; Yeh & Schum, 1980). Nevertheless, the regularly bifurcating model (often referred to as the 'trumpet model') has been of great utility for the basic computation of aerosol deposition estimates. More recently, 1D computational models such as MPPD can utilize CT imaging to truly represent the asymmetry of the morphometry of the upper airways while retaining the assumption of regular bifurcation of distal airways, which are so small that imaging cannot resolve them. Rather than using the assumption of regular bifurcation for distal airways, the approach of Tawhai uses the imageable lobar geometry to generate a hypothetical morphometry of the distal airways (Tawhai et al., 2004; Tawhai, Pullan, & Hunter, 2000).

Multiscale models of the lung can represent natural breathing driven by time-dependent modification of intrapleural pressure due to contraction of the diaphragm and chest muscles. Similarly, they can represent artificial ventilation driven by external pressure-driven flow at the mouth during inhalation and natural exhalation due to unassisted chest wall and diaphragmatic elastic recoil (Fig. 1A). Alternatively, they can model flows by imposing flows as derived from lung volume changes by comparing multiple CT images taken during the breathing cycle (Fig. 1B). Multiscale models can employ 3D CFPD models in proximal regions (typically the URT (upper respiratory tract) and the first 3–5 generations of airways in the lung) with connection to attached lower dimensional airways, which include the alveolated respiratory airways.

Alternatively, modeling with 3D CFPD in upper airways can be done to derive artificial intelligence/machine learning (AI/ML) models that can be used to inform and adjust lower-dimensional models that can then be run in much faster time than the models having a 3D CFPD component (Choi et al., 2019; Zhang et al., 2022). This is a multiscale approach that ultimately uses only lower-dimensional models in the final product (Fig. 2). Conversely, 3D models can be employed to simulate all scales of the lung assuming only one or more typical paths to the alveoli. They employ assumed self-similarity of the airways at all intermediate generations (Fig. 3).

2.3.2.1. Multiscale models driven by natural or mechanically ventilated breathing. When driven by an intrapleural or mouth pressure waveform (Figs. 1A), 3D/0D interfaces must match the flows and pressures on each side of the interface, i.e., coupling needs to be achieved between a 3D finite element or volume code and ODEs representing the distal lung (Ismail et al., 2013; Ismail, Gravemeier, Comerford, & Wall, 2014; Kuprat, Kabilan, Carson, Corley, & Einstein, 2013; Oakes et al., 2014).

Ismail and colleagues achieved such coupling with the stabilized Petrov-Galerkin finite element method (Ismail et al., 2014). At each time step, iterations were performed to stably establish pressure and flow values that agreed between the 3D domain and the domain described by ODEs. It was emphasized that when flow was from the 3D domain to the 0D domain, stability would require agreement between hydrostatic pressure of 3D and 0D domains. When flow was reversed back into the 3D domain from the 0D domain, stability requires agreement of total momentum flux (i.e., total pressure which includes sum of hydrostatic pressure and dynamic pressure) between the two domains. In that paper, coupling of a human geometry with 5 outlets (i.e., one per lobe) was stably achieved. The method developed by Moghadam et al. (Moghadam, Vignon-Clementel, Figliola, & Marsden, 2013) was employed by Oakes et al. (Oakes et al., 2014) to couple a 3D finite element code and ODEs representing the distal lung. Here, flow was driven by tracheal pressure in an intubated rat. In (Oakes et al., 2017), the same coupling was used, but the resultant 3D/0D interfacial flow was used to drive a 1D PDE in each of 5 rat lobes that represented the distal lobar domains with flow and airway cross-sectional area as functions of continuous axial distance parameter z rather than discrete airway generation index i. Deposition in the 1D domain was also computed as a function of downstream distance z with deposition functions for inertial impaction and gravitational sedimentation.

Finally, in (Kuprat et al., 2013), analogous coupling was performed between the open source finite volume CFD solver OpenFOAM

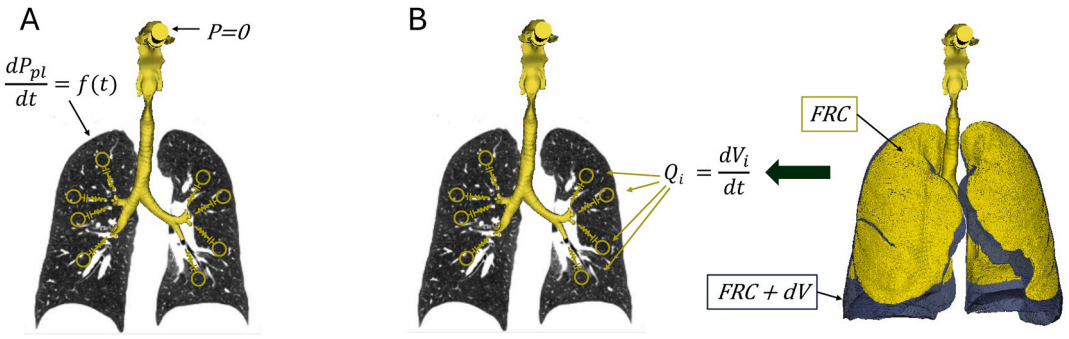

Fig. 1. Subject-specific multiscale models. A: model driven by prescribed time-dependent intrapleural pressure, with continuity of pressure, flow, and particle flux at 3D/1D interfaces. In case of mechanical ventilation, driving pressure can be specified at the mouth. B: model driven by 3D/1D interface flows determined by volume differences in CT images taken at different times in the breathing cycle.

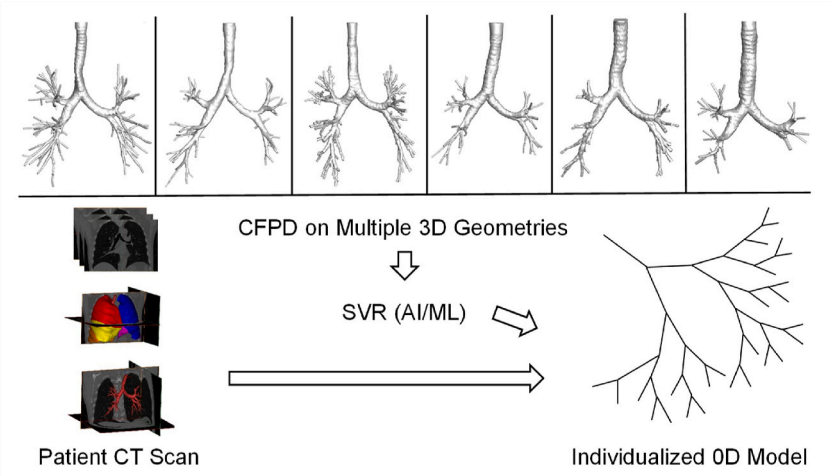

Fig. 2. Patient-Specific 1D model for rapid dosimetry calculation, aided by machine learning which adjusts airway deposition factors based on 3D features appearing in patient CT scan.

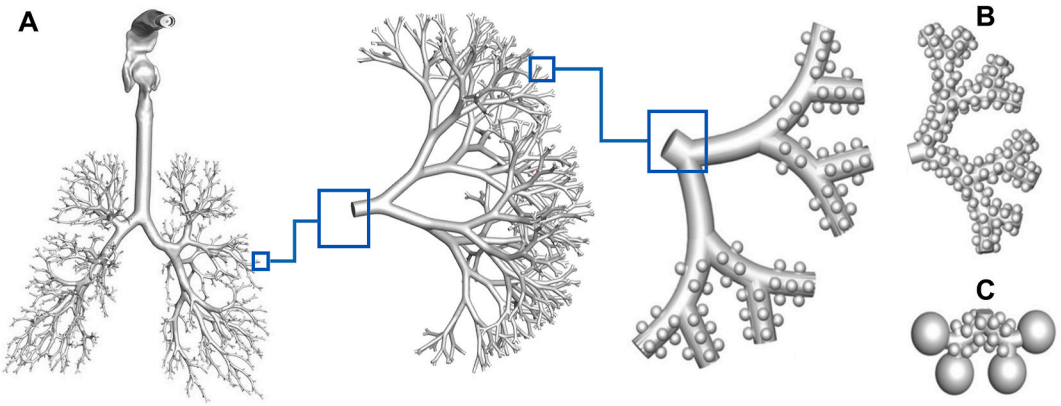

Fig. 3. Fully 3D computation using two typical paths (for left and right lung, A), driven by moving alveoli. Computation is sped up by using self-similar triple bifurcation unit (B) and terminal double bifurcation unit (C).

and the attached ODEs by equating hydrostatic pressure during inhalation (with flow exiting the 3D domain into the distal 0D domain), while total pressure was equated during exhalation when the flow was reversed and entered the 3D domain from the 0D domain. As 117 distal ODE outlets were attached to the 3D domain (a CT-based human geometry containing oral cavity, larynx, and tracheobronchial tree), a Krylov subspace method was used to avoid expensive computation of the full Jacobian matrix for convergence of iterations at each time step. It was found that, to achieve a stably converged subiteration at each timestep of the pressure and flow variables, iteration of interface pressure to equate pressure drop over the connecting segment was necessary, as opposed to simply iterating interface pressure to equate flow. As shown in the Appendix of (Moghadam et al., 2013) using a similar approach for cardiovascular applications, iterating over the interface pressure to equate flow is unstable if the connection between 3D and 0D starts with a 'capacitor' or 'inductor'. This is the case when the connecting airway segment is modeled as having compliance or inertance. With each most distal airway of the 3D domain, the equating of pressure and pressure drop between the 3D domain and the 0D domain effectively enforced the conservation of flow to a high degree.

2.3.2.2. Multiscale models driven by CT-imaged lung volume changes. Recently, the availability of patient-specific lung images at two time points, such as the end of a normal exhalation (i.e., functional residual capacity (FRC)) and end of inhalation (FRC + tidal volume (TV) or total lung capacity (TLC)) allows for determining flows out of each distal outlet of the 3D domain (De Backer et al., 2010; Kuprat et al., 2023). The experimentally observed flows at the 3D outlets give realistic subject-specific flow data where the individualized airway subtrees distal to each 3D outlet may have flows that deviate from healthy lungs due to disease.

Kuprat and colleagues (Kuprat et al., 2021, 2023) used CT lung images of a healthy subject obtained at FRC and FRC + TV to determine flows into 11 distal airways of the subject-specific airway model (Fig. 1B). *In silico* simulations were set to match experimental conditions of aerosol exposure in the same subject from which the lung model was developed (Darquenne, Lamm, Fine, Corley,

& Glenny, 2016). In the experimental study, the subject was asked to target a tidal volume of 1000 ml of particle-laden air (1 and 2.9 μm, respectively) at constant inhalation flow rates of 300 (slow breathing) and 750 ml/s (fast breathing). This made for 4 different simulations using subject-specific tidal volumes and flow rates where the retained fraction of particles could be compared with experimentally measured values. For these simulations, the lung distal to each outlet of the 3D CFPD model was modeled as a bi-directionally coupled 1D subtree, for which particle transport and deposition were calculated using the latest version of the MPPD model (Asgharian et al., 2022). In the 3D domain, flows were specified at the distal outlets. Zero total pressure was specified at the proximal inlet of the 3D domain. Flows were passed to the distal MPPD subtrees, along with time-dependent particle fluxes exiting the 3D domain. During exhalation, the continuum particle concentration exiting the MPPD subtrees was converted to a corresponding concentration of Lagrangian particles that were injected and tracked into the 3D portion of the domain. Using this approach, Kuprat et al. (Kuprat et al., 2023) noted good agreement between *in silico* predictions and experimental values of retained fractions. They also showed that while particles inhaled in subregions of the lung (as computed by the 3D CFPD model) were roughly proportional to (CT image-derived) flows into these sub-regions (Fig. 4A), regional particle retention greatly deviates from regional ventilation (Fig. 4B).

2.3.2.3. Multiscale models utilizing machine learning for faster execution. In (Zhang et al., 2022), the need for coupling 3D CFPD to a lower-dimensional model is avoided by running a 3D code multiple times on airways that deviate from a cylindrical shape to create deposition enhancement factors. These factors estimate how deposition in the airway is altered compared to one-dimensional models that assume a perfect circular cross section. The information gathered is stored using SVR (Support Vector Regression), which is a form of AI/ML. Then, a CT image of the subject, which shows 3D features of airways, can allow for the generation of a tuned 1D code that uses the encoded SVR deposition enhancement factors. Additionally, by comparing two images taken at FRC and TLC, subject-specific flows are inferred from volume changes between the images. Non-imaged distal airways are generated by using the space-filling algorithm of Tawhai (Tawhai, Pullan, & Hunter, 2000) in each lung lobe. A fully one-dimensional model models the whole lung (starting at trachea) down to the last respiratory generation. The enhancement factors correct deposition in the proximal airways where airway shapes can be imaged, while localized flows inferred by the difference in the FRC and TLC images drive flow in the last generation of the 1D flow model of Choi et al. (Choi et al., 2019). Small particle sizes of order ~0.01 μm deposit mainly by diffusion, while larger particle sizes of order 10 μm deposit mainly by sedimentation and impaction. For these particle sizes, the enhancement factor did not change predicted deposition significantly. However, for intermediate-sized particles of order 0.1–1 μm, enhancement factors determined by patient-specific imaged lung morphology significantly increased deposition in the proximal airways due to the mechanisms of enhanced laminar diffusion and sedimentation. Thus, this technique has the potential of 'front-loading' the 3D modeling work to inform a smart, fully 1D model that can be run much faster than a hybrid 3D/1D model. This could be of significant use in clinical settings where simulations should ideally take as little time as possible to run. The study of (Zhang et al., 2022) was limited to a small cohort of COPD patients and was validated using CT/SPECT imaging data. It was noted by the authors that further validation of their technique was needed for predicting deposition in the case of other diseases such as asthma, since structure and function of the lung differ with different diseases.

2.3.2.4. Fully 3D typical path model using self-similar meshing. In (Kolanjiyil & Kleinstreuer, 2017), the need for coupling of 3D to lower-dimensional code is avoided by modeling two typical paths (corresponding to left- and right-lungs) using the 3D finite volume commercial code Ansys CFX for solving the Navier-Stokes equations with SST $k-w$ turbulence model (down to generation 6) and Lagrangian particle transport. The URT and first 3 generations are modeled with a patient-specific geometry, and then the distal generations are modeled with bifurcations in a self-similar fashion using identical but increasingly smaller scaled triple bifurcation units (TBU) (Fig. 3). These two typical paths are extensions of the median diameter outlets at generation 3 of the left- and right-lung. The last two generations (22–23) of the respiratory system are modeled using a double bifurcation unit (DBU). Spherical alveoli are attached to respiratory airways. URT and triple bifurcation units are modeled as fixed, while flow is driven by 3D movement of

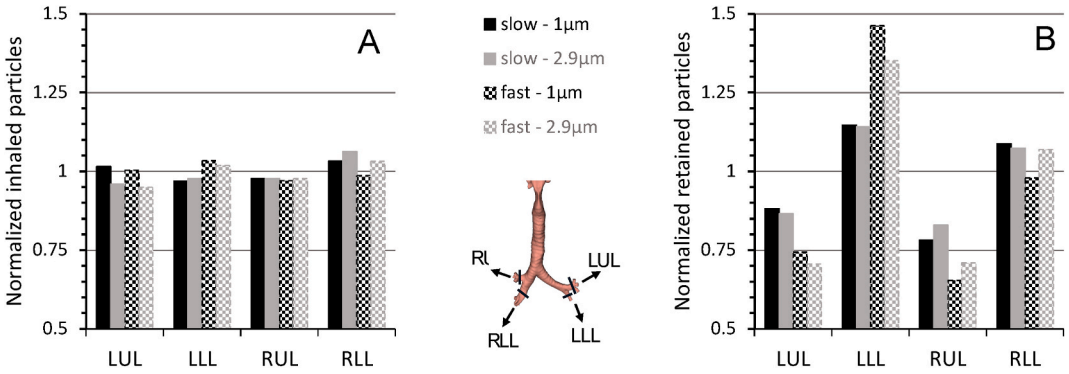

Fig. 4. *In silico* predictions as calculated in (Kuprat et al., 2023) from a subject-specific multiscale model of a 35-year-old healthy adult male. A: Predicted particle inflow in each subregion relative to CT image-derived inflow. B: Predicted retained particles relative to subregion inflow. LUL: left upper lobe, LLL: left lower lobe, RUL: right upper lobe, RLL: right lower lobe. Note that, for this subject, there was an incomplete oblique fissure between the middle and inferior lobe and both lobes were merged in this analysis.

spherical alveoli and the double bifurcation unit comprising the last generation. The 3D code solved the typical paths with very large timesteps (dt = 0.05s) due to the optimally meshed TBUs which were self-similarly meshed (Bronchiolar TBUs had 500k elements and alveolar TBUs had 2 million elements). However, it should be noted that the assumption of symmetrical and self-similar bifurcating airways deviates from actual human airways, which can be asymmetrical. In addition, the displacement function for the alveolar geometries had to be predetermined, rather than being driven by an assumed intrapleural pressure waveform. Nevertheless, it seems that in principle with some assumptions on the compliance of the alveoli, the model could be driven by changes in transmural pressure. Deposition of particles was modeled by the Lagrangian method and showed reasonable agreement with experiments, with predictions of overall deposition underestimating experimental data by ~15–20% (relative change). Generalization to 5 paths (i.e., one for each lobe) is also possible.

Other works employing self-similar 3D geometries include that of (Rahman, Zhao, Islam, Dong, & Saha, 2022), applied to 5 nm–20 nm particles, and that of (Koullapis et al., 2018, 2020), applied to 0.1um to 10um particles. Although the Rahman model ends in the conducting zone, the Koullapis model continues into a heterogeneous 3D model of a sub-acinar unit based on a Voronoi tessellation of seed points (Koshiyama & Wada, 2015). The airflow is then driven by isotropic expansion and contraction of the sub-acinar unit as in (Hofemeier, Koshiyama, Wada, & Sznitman, 2018).

Finally, the stochastic individual path (SIP) model (Longest et al., 2019; Tian, Longest, Su, Walenga, & Hindle, 2011) utilizes similar 3D meshes, to discretize generations down to the terminal bronchioles (generation 15), but only continues each airway into one of two daughter branches in each subsequent generation. Each daughter is randomly chosen unless choice of one of the daughters would cause the path to impinge on the lobar boundary, in which case the choice of the other daughter is forced. It is noted that in principle multiple stochastic individual paths can be generated within each lung lobe until lobar deposition results are deemed to have converged. Also, by using a fully 3D simulation, 3D effects potentially important to medical inhalers used in respiratory drug delivery such as jet momentum and particle evaporation can be dealt with using 3D physics, avoiding assumptions inherent in 1D deposition models that may not apply for the device/aerosol combination. Modeling of metered dose inhaler and dry powder inhaler aerosols was conducted using SIP in (Walenga & Longest, 2016). Also, SIP modeling was continued into the respiratory zone in (Khajeh-Hosseini-Dalasm & Longest, 2015) by representing alveoli using space-filling 14-sided polyhedra that deform isotropically to ventilate the lung.

3. Multiscale models – PBPK models

3.1. Introduction to PBPK models

Physiologically-based pharmacokinetic modeling seeks to evaluate the absorption, distribution, metabolism, and excretion (ADME) of toxic or medicinal chemicals in one or more compartments of humans or animals. Compartments can include blood, liver, lungs, gut, and others as required for modeling the relevant organs affected by the delivered substance. Typically, distribution into a compartment is rate-limited by blood flow, giving the following expression for time-dependent concentration $c(t)$ in a compartment:

$$V \bullet \frac{dc}{dt} = Q(t) \bullet \left(c_{blood}(t) - \frac{c(t)}{P} \right) - V \bullet r(t) + S(t) \tag{4}$$

Here, V is the volume of the compartment, $Q(t)$ is the blood flow into the compartment, $c_{blood}(t)$ is the concentration of the blood entering the compartment, P is the tissue:blood partition coefficient of the substance in the compartment, $r(t)$ is loss rate due to metabolism, and $S(t)$ represents a compartment-specific source (or sink) such as oral ingestion, inhalation, renal elimination, etc. The partition coefficient is necessary since only a fraction $1/P$ of the substance is dissolved in the blood of the compartment and is thus able to be washed out by the blood flow. The loss rate could represent metabolism by zeroth order, first order, and saturable Michaelis-Menten kinetics:

$$r(t) = k \quad ; \quad r(t) = k \bullet c(t) \; ; \quad r(t) = \frac{V_{max} \bullet c(t)}{K_m + c(t)} \tag{5a-c}$$

PBPK models thus represent a set of compartment ODEs that are connected by blood flows and which have specific sources and sinks corresponding to the routes of exposure and elimination of substances. For a bolus or chronic exposure to a substance, PBPK models typically evaluate the maximum concentration (C_{max}) and the AUC ("Area under the curve") for one or more specific compartments or blood plasma concentration. For bolus exposure, the MRT ("mean residence time") is also evaluated. AUC and MRT are defined by:

$$AUC = \int_0^\infty c(t)dt \tag{6}$$

$$MRT = \frac{\int_0^\infty t \bullet c(t)dt}{\int_0^\infty c(t)dt} \tag{7}$$

C_{max}, AUC and MRT are considered important quantitative measures of the overall exposure to the drug or toxin and of its persistence in the body (Kwon, 2001). Thus, evaluation of these quantities can be considered to be important goals of exposure modeling.

PBPK models are available for animals as well as humans. Comparing C_{max} and AUC for experimental animal and hypothetical human exposures (with PBPK models for each species adjusted for differing anatomy and physiology) can create a more reliable method of predicting the effect on humans of an experimental chemical exposure. See for instance (Corley et al., 2012, 2015) for predicting the human equivalent dose corresponding to experimental observations of effects in animals for aldehydes (acrolein, formaldehyde, and acetaldehyde).

In the case of inhaled drugs or toxins, PBPK models have typically considered the lung as a single compartment with no distinction between URT, conducting airways, and the alveolar region. Clearly exposure in these different areas can have important consequences on the fate of the substance. For example, substances that deposit in the conducting airways will be largely cleared from the lung via the mucociliary escalator on a relatively short time scale, while substances depositing in the alveoli can remain in the lung tissue for much longer or even translocate to the heart. Also tissue cells in the different regions of the lung can have different susceptibility to toxic effects or may or may not represent the intended targets of drug exposure. More recently GastroPlus™ and SimCyp Simulator™ PBPK models support division of the lung into multiple compartments (Bäckman et al., 2018). Coupling of CFPD code with PBPK models can give important spatial-specific exposure information, which can be of use in ultimately evaluating the effectiveness of a medical exposure. Taking into account the areas of deposition of particles and vapors (i.e., by breaking the lung into several spatially separate compartments introduces a modeling dependence on patient-specific airway geometry (Fig. 5) (Feng, Zhao, Hayati, Sperry, & Yi, 2021). Thus, coupled CFPD/PBPK modeling has the potential of giving patient-specific information for optimizing inhaled drug therapy outcomes.

3.2. Introduction to CFPD-PBPK models

For many materials, understanding where aerosols deposit is only the first of potentially several key events necessary to predict a dose metric that is relevant to a material's mode of action (MOA). For poorly soluble aerosols, mucociliary transport or phagocytosis by macrophages or dendritic cells may be important processes to address to determine cleared vs. retained doses following deposition in the respiratory system. Clearance models, such as that of the ICRP (ICRP, 2015) which has been applied to CFPD simulations (Corley et al., 2021) and those incorporated within MPPD (https://www.ara.com/mppd/) are examples of modeling tools available to understanding retained dose over time following single or multiple exposures for these poorly soluble materials.

For aerosols that may be soluble enough to be absorbed and transported within airway tissues or reach systemic blood circulation before mucociliary or other clearance processes remove them from the airway surfaces, other types of models have been used in conjunction with CFD-based simulations to improve predictions of biologically relevant doses for a given MOA. For example, mass-transfer and tissue reaction kinetics have been incorporated as boundary conditions for nasal airway CFD models of the rat, monkey, and/or human to predict local tissue doses of reactive gases or vapors such as methyl methacrylate, formaldehyde, chlorine, hydrogen fluoride, ozone, sulfur dioxide and xylene (Andersen & Sarangapani, 2001; G. J. Garcia, Schroeter, et al., 2009; Kimbell & Subramaniam, 2001). CFD simulations of airflows in nasal airways have also been used in hybrid CFD-informed physiologically based pharmacokinetic (PBPK) models for these and other reactive gases or vapors such as acrolein, acetaldehyde, ethyl acrylate, and hydrogen sulfide (Andersen & Sarangapani, 2001; Andersen, Sidaros, Gesmara, Rostrup, & Larsson, 2000; Bush, Frederick, Kimbell, & Ultman, 1998; Corley et al., 2009; Frederick et al., 2001; Schroeter et al., 2008; Schroeter, Kimbell, Bonner, et al., 2006; Sweeney, Andersen, & Gargas, 2004). As CFD-based models for locally toxic gases and vapors became more widespread, multiscale, fully coupled CFD/PBPK models have been developed for a variety of locally toxic vapors (Corley et al., 2012, 2015; Morris & Hubbs, 2009; Schroeter et al., 2013; Schroeter, Kimbell, Andersen, & Dorman, 2006). More recent models are discussed in the section below.

3.3. Current CFPD-PBPK models

Since 2018, there have been several papers using CFPD-PBPK models to investigate two major topics, i.e., (1) the evaluation and optimization of inhalation therapy and pulmonary healthcare (Dave, Kleinstreuer, & Chari, 2022; Haghnegahdar, Zhao, Kozak, Williamson, & Feng, 2019; Kannan, Singh, & Przekwas, 2018; Ladumor & Unadkat, 2022; Sperry, Feng, Song, & Shi, 2024; Vulović, Šušteršič, Cvijić, Ibrić, & Filipović, 2018; Zhao, Feng, Tian, Taylor, & Arden, 2021), and (2) the exposure risk assessment on airborne toxicants (Haghnegahdar, Feng, Chen, & Lin, 2018; Kuga & Ito, 2019; Kuga, Ito, Chen, Wang, & Kumagai, 2020; Yoo & Ito, 2018a,

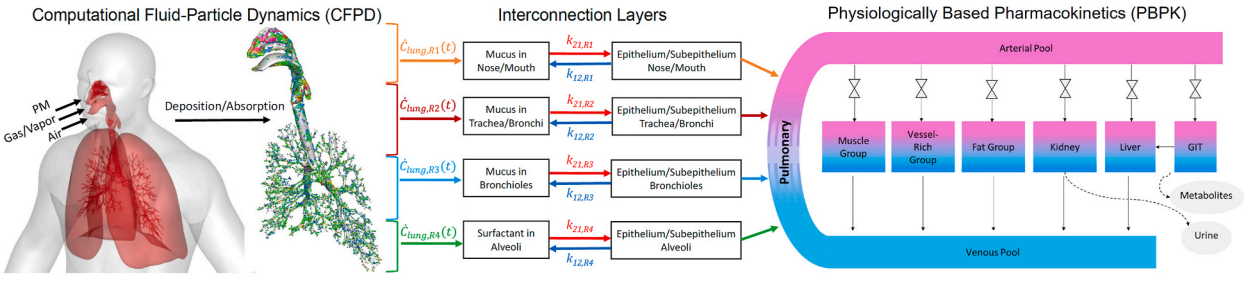

Fig. 5. CFPD/PBPK Modeling. CFPD model with several patient-specific lung compartments distributes chemical fluxes into PBPK simulation with other affected body compartments. From (Feng et al., 2021).

2018b). Integrating CFPD with PBPK models allows for a more comprehensive understanding of how inhalable particles behave within the human body, especially in the lungs, and how this relates to pharmacokinetics and toxicokinetics.

3.3.1. *Evaluation and optimization of inhalation therapy and pulmonary healthcare*

Kannan et al. (Kannan et al., 2018) employed a Quasi-3D Compartmental Multiscale CFPD-PBPK model (Q3D) for inhaled budesonide absorption, transport, and retention in the human lungs. The authors claimed their model represents a substantial step forward in optimizing target-specific drug delivery and enhancing drug bioavailability in lung disease treatment. It improves over traditional 0D compartmental models and high-fidelity CFD models by enabling the prediction of drug delivery considering different localized bioavailability factor values, thereby facilitating applications for various patient and lung disease conditions. Their CFPD-PBPK model preserves 3D lung geometry, which allows for modeling heterogeneous annular lung layers, enabling detailed drug transport across these layers. However, in the current Q3D model, the accuracy for capturing complicated secondary flows and detailed features could be improved.

Vulović et al. (Vulović et al., 2018) used a combined CFD-PBPK model for predicting the aerosolization, deposition, and absorption of Amiloride Hydrochloride, a drug used for treating edema related to various conditions, delivered through a dry powder inhaler (DPI). Their model offers a detailed simulation of how the actuated airflow condition can influence the emitted drug dose from the DPI and drug plasma concentration. Improvements could be made in (1) integrating the discrete element method (DEM) to model the particle-particle interactions accurately, and (2) employing a physiologically realistic airway geometry to predict the aerosol transport dynamics in a more physiologically realistic lung environment. Specifically, the particle size distribution and particle transport dynamics will not be accurate without considering the agglomeration and deagglomeration between particles especially in DPI, which can be effectively modeled using CFD-DEM (Zhao et al., 2022). Additionally, employing physiologically realistic airway geometry allows for more accurate and personalized predictions of lung dosimetry for inhaled drug particles. With such improvements, the CFD-PBPK model can serve as a high-fidelity tool to evaluate the performance of DPIs to optimize the drug delivery efficiency for inhalation therapy.

Zhao et al. (Zhao et al., 2021) and Sperry et al. (Sperry et al., 2024) employed an experimentally calibrated CFPD-PK model to analyze the transport, deposition, and translocation of inhaled aerosolized medicinal cannabis in multiple 3D human respiratory system geometries. Their studies focused on how anatomical differences and inhalation techniques affect PK profiles, which is crucial for assessing pain relief effectiveness and overdose risks. Although their simplified 3-compartment PK model offers insights, it suggests a potential upgrade to a more detailed PBPK model for better prediction across different tissue groups, which can provide a more detailed analysis of therapeutic effectiveness or overdose risk. Additionally, the use of bioavailability factors, though experimentally optimized, highlights a need for more refined modeling of airway-blood interactions, paving the way for a more comprehensive CFPD-PBPK framework.

Haghnegahdar et al. (Haghnegahdar et al., 2019c) evaluated the safety of inhaled Xenon and its anesthetic effectiveness using a CFD-PBPK model with a unique interconnection model, i.e., TRANSIT, to consider the dampening effect of the tidal discharge of the gas into the systemic region induced by the presence of the epithelial and sub-epithelial layers. Future enhancements to the CFD-PBPK model and anesthetic effect studies should encompass several key areas: integrating thermodynamics and bio-reactions at airway tissue sites for improved drug interaction simulations; investigating the variability in drug effectiveness and health risks between healthy individuals and patients with restrictive or obstructive lung diseases, focusing on xenon and other pulmonary drugs; employing a whole-lung model for more accurate drug deposition and absorption analysis; and incorporating nasotracheal or tracheal intubation tubes into the model's geometry to reflect their use in maintaining an open glottis during anesthesia, which significantly impacts drug delivery dynamics.

Slightly different from the above-mentioned multiscale modeling effort, Ladumor and Unadkat (Ladumor & Unadkat, 2022) integrated the ICRP and PBPK model with a unique interconnection model to predict the dose of the orally inhaled (OI) drug delivered to different tissue groups in the human body. Specifically, the ICRP model was used to predict lung deposition of the OI drug. In contrast, the unique interconnection model explicitly simulated the transport of drugs in the epithelial lining fluid (ELF), epithelial and sub-epithelial layers between the airway lumen, and blood.

Finally, Dave et al. (Dave et al., 2022) focused on improving the understanding of the performance of nasally administered drugs. It uses CFPD-PBPK modeling to simulate the behavior of inhaled corticosteroids. The paper provides a detailed view of drug aerosolization, deposition, absorption in the nasal mucus layers, and subsequent migration from the nasal cavity to the bloodstream.

3.3.2. *Exposure risk assessment on airborne toxicants*

CFPD-PBPK models have also been increasingly used in environmental and occupational health studies to assess the risk of exposure to pollutants and other airborne particles/vapors, mostly focusing on aerosol species emitted from e-cigarettes.

Haghnegahdar et al. (Haghnegahdar et al., 2018) developed a perfusion-limited CFPD-PBPK model and simulated how inhaled nicotine and acrolein transport and translocation are influenced by puff topography features during e-cigarette exposure and use. This study employed an idealized mouth-to-generation 3 (G3) airway model. The coagulation, condensation, and evaporation among particle and vapor phases were not modeled. The interconnection model between the airway lumen and bloodstream should also be developed for different pulmonary regions to reflect the different diffusion and reaction characteristics in those regions.

Yoo and Ito (Yoo & Ito, 2018a; 2018b) developed a CFD-PBPK model combining a virtual indoor environment and a 3D virtual human model to simulate the transport and translocation of formaldehyde from indoor environments to the human respiratory system, and subsequently to the mucus, epithelium, and subepithelium layers. The PBPK model specifically addresses the mucus + epithelium and subepithelium layers. This innovative approach allows for accurate predictions of exposure levels near the mouth and nose using

first principle based governing equations of conservation laws of mass, momentum, and energy, as well as the advection-diffusion species transport equation, based on varying indoor ventilation conditions. However, to enhance the modeling scope, it is essential to expand the CFPD-PBPK modeling capabilities to predict translocation to multiple tissue groups throughout the human body after reaching the subepithelium layers, thereby extending its predictive power to all relevant health endpoints.

Utilizing the established CFPD-PBPK modeling framework, Kuga and Ito (Kuga et al., 2020; Kuga & Ito, 2019) expanded their research to examine the transport and translocation of various e-cigarette aerosol components, including formaldehyde, acetaldehyde, acrolein, benzene, toluene, glycerol, and nicotine. Their study traced the journey of these substances from indoor spaces to a limited respiratory tract model (i.e., from mouth and nose to the 4th bifurcation) with subepithelia. A key focus of their investigation was on the impact of puff topography on exposure levels in the head region, the delivered dose within human respiratory systems, and dermal exposure levels. This comprehensive approach provided deeper insights into the influence of inhalation patterns on the predicted distribution and impact of e-cigarette aerosols on human health.

In summary, continuous research has been made on developing advanced integrated CFPD-PBPK models, due to several advantages over single PBPK models. First, integrated CFPD-PBPK models provide a more holistic analysis of aerosol transport, deposition, and translocation in the physiologically realistic respiratory system environment and the whole body. This is vital for assessing therapeutic or toxicokinetic effects more precisely. Second, the CFPD-PBPK models can offer more accurate predictions for specific subjects or disease conditions, including variations due to extrinsic and intrinsic factors in lung environments and pulmonary airflow dynamics variations. Therefore, physiologically realistic CFPD-PBPK modeling efforts and applications can simulate clinical outcomes in studies where enrollment is challenging or where there are ethical considerations, thereby potentially reducing the need for human subjects. Thus, there is a growing trend towards using these CFPD-PBPK models for personalized medicine. By considering individual physiological differences, models can predict how specific patients might respond to inhaled drugs. However, the challenge lies in how to model the interconnection layer between airway lumen and blood in a physiologically realistic and accurate way.

3.4. Subject-specific modeling considerations

3.4.1. Importance of personalized or subject-specific modeling in respiratory health

One of the potential benefits of employing a CFPD-PBPK model instead of a PBPK-only model is the capability of capturing the subject-specific variabilities in pulmonary air-particle flow dynamics, i.e., anatomical features of pulmonary airway topology, breathing patterns, etc., which will lead to variabilities in lung dosimetry of inhaled aerosols, together with the individualized absorption, distribution, metabolism, and excretion (ADME). Specifically, to achieve uncertainty quantification and make the computational model more statistically representative, variability factors must be considered in simulations. The initial variability factors prior to ADME variabilities are the variations in human anatomy and physiology, which play a critical role in the deposition and distribution of inhaled aerosols, directly influencing the resultant PKs in systemic regions. Subject-specific modeling enabled by CFPD facilitates the capture of these variances, particularly in the topology of pulmonary airways and the diversity of breathing patterns among individuals. This capability is crucial for accurately predicting lung dosimetry of inhaled aerosols (Feng et al., 2018a), which is important in the assessment of exposure safety. By incorporating subject-specific variabilities, CFPD-PBPK models enhance our understanding of how inhalable aerosols interact within the respiratory system, enabling personalized occupational risk assessment and prevention.

3.4.2. Techniques for tailoring models to individual physiological differences

To achieve subject-specific modeling using CFPD-PBPK to capture the individual physiological differences, there are three standard categories, as follows.

3.4.2.1. Category 1: construct subject-specific body surfaces and airway geometries for CFPD simulations. Current advancements in imaging technology and computational capabilities have paved the way for the development of realistic, subject-specific models of the human body external surface (https://humanshape.org/) (Chen & Zhao, 2010; Gupta, Lin, & Chen, 2011; He, Niu, Gao, Zhu, & Wu, 2011; Li, Shang, Yan, Yang, & Tu, 2018; Yang, Kang, Hwang, & Park, 2017; Zhang & Li, 2012; Zhao, Feng, Bezerra, Wang, & Sperry, 2019; Zhu, Kato, & Yang, 2006) and respiratory system (i.e., virtual human models). These models are essential for conducting detailed studies on airflow and the transportation and deposition of inhaled aerosols within the respiratory tract. This marks a significant shift from the earlier reliance on idealized airway geometries to employing detailed models that accurately reflect individual anatomical variations. The process of constructing subject-specific virtual human models requires the use of high-resolution 3D medical images from which the detailed anatomy of the respiratory system is isolated through a process known as segmentation. This involves identifying and outlining the body shape and airways, separating the lung lobes, and refining the model to ensure it represents a coherent, singular anatomical structure. The refined model is then converted into Stereolithography (STL) format, compatible with the mesh generation tools used in computational simulations.

Such construction benefits from various image processing software, including Amira, Simpleware ScanIP, and Materialise Mimics. Moreover, repositories of CT and MRI scans (Clark et al., 2013; COPDgene, 2019; NBIA, 2019) offer a wealth of data that can be utilized to incorporate variability in airway structure between different subjects into these models. However, it is also worth noting that reconstructing subject-specific airway geometries needs to be done cautiously to guarantee accuracy, which can be significantly influenced by the medical imaging process and its associated radiation doses.

3.4.2.2. Category 2: integrate subject-specific exposure and breathing conditions into CFPD simulations. Other than the variabilities in the anatomical features of the human body, such as shape and respiratory system, subject-specific exposure conditions, breathing conditions, and other lung properties can also significantly induce variability in inhaled aerosol transport and deposition. These factors can include.

(1) Exposure levels (i.e., aerosol concentration) around the head region or mouth/nose openings for certain individualized exposure conditions, aerodynamic particle size distributions (APSDs), particle shape, particle surface properties,
(2) Breathing conditions including breathing waveforms with key features such as average inhalation flow rate, inhalation duration, breath holding duration, exhalation duration, and
(3) Lung mechanical properties such as lung compliance.

These factors can be employed as subject-specific initial conditions, boundary conditions, and material properties in fluid-structure interaction (FSI) to enable subject-specific CFPD simulations.

3.4.2.3. Category 3: model subject-specific ADME in PBPK simulations. The modeling of subject-specific ADME processes within PBPK simulations should integrate individual physiological and biochemical parameters, which can be obtained from benchmark clinical studies or animal studies. PBPK models can predict how individuals with distinct genetic backgrounds, health conditions, or age groups metabolize and respond to various substances. This individualized approach allows for the simulation of chemical concentration-time profiles and the personalized assessment of exposure risk. However, advancements in integrating such detailed individual data into PBPK models require addressing current data limitations, such as the availability of comprehensive population-specific protein expression data and a detailed understanding of lung-specific drug metabolism (Enlo-Scott, Bäckström, Mudway, & Forbes, 2021; Oesch, Fabian, & Landsiedel, 2019). Methodological complexities, including the development of robust techniques for integrating diverse biological data and modeling the dynamic interactions within the lung microenvironment, also need to be overcome to achieve accurate and reliable predictions in personalized PBPK modeling.

3.4.3. Impact of subject-specific modeling on predictive accuracy and clinical relevance

Adopting subject-specific CFPD-PBPK models in respiratory health research will provide more accurate predictions for occupational exposure risk assessment with uncertainty quantifications on the variabilities between individuals in airway physiology, exposure and breathing conditions, and ADME processes. Specifically, the subject-specific modeling strategy provides the potential for generating more precise predictions of aerosol transport, deposition, and translocation within the lungs and in systemic regions. Such enhanced predictive accuracy will have significant clinical relevance, as it enables personalized risk assessment and the customization of preventive care or therapies to meet the specific needs of each subject. In conclusion, subject-specific modeling, particularly through CFPD-PBPK models, significantly advances occupational exposure risk assessment and pulmonary healthcare. By enabling the detailed analysis of individual variances in pulmonary air-particle flow dynamics and PK predictions, the continued development and refinement of these models will have significant impacts.

3.5. Challenges and prospects in enhancing current CFPD-PBPK models

CFPD-PBPK modeling faces challenges that are being overcome for practical use in predicting or explaining the effects of drugs or toxicants.

CFPD. Ideal deposition of spherical particles in typical geometries of neonatal, children, and adults of both sexes has been widely performed. However, this is a first step. Particles can be non-spherical, leading to enhanced deposition and enhanced negative effects in the case of toxic particles (Kleinstreuer & Feng, 2013). Correct modeling of deposition depends on categorizing the density, shape, and possible cloud behavior of these particles. Modeling of clearance by the mucociliary elevator can be uncertain due to the possibility of impairment of the lung cilia by the inhaled substance (Palazzolo et al., 2017). Research is ongoing on the effect of airway diseases such as asthma and COPD on the initial distribution and clearance of inhaled particles.

Interconnection between CFPD and PBPK. In general, the cost of CFPD modeling greatly exceeds that of PBPK modeling as it is a 3D computation compared to a system of ODEs. The interconnection is relatively inexpensive and convenient as the relatively expensive results from CFPD modeling are then distributed into a small number of lung PBPK compartments as source and sink terms in the PBPK ODE model. Thus, CFPD/PBPK modeling can, in general, be expected to be little more expensive than stand-alone CFPD modeling.

PBPK. Setting or updating the large number of parameters in PBPK models can be difficult. An expensive option is initiating a new clinical trial with the specific drug and target population by fitting the parameters of the PBPK system to the observed results. It should be noted that pharmacodynamic (PD) models that describe the effect of medications on the body once they are delivered to the tissues as predicted by PBPK models would have to be updated as well. Indeed, in certain cases, blinded clinical trials are not possible due to ethical considerations. However, there is an increasing base of 'system' parameters that are generally known, such as rates of blood flow into different organs and how they depend on age and gender. Non-proprietary information is shared in the literature, leading to standard models of how different drug classes are perfused or diffused between various compartments of the body. Missing information can be obtained from *in vitro-in vivo* extrapolation (IVIVE) and testing and optimizing missing PBPK parameters by accessing and even reanalyzing existing clinical trials on related drugs that have similar mechanisms of action (Rostami-Hodjegan, 2018).

A new development for accumulating patient specific data involves the construction of a 'digital twin' for a patient representing a

PBPK/PD model customized to *a priori* knowledge of the individual via genetic testing and patient health data, and then augmented during the course of treatment by recorded responses to therapy during regular patient visits (Fischer, Volpert, Antonino, & Ahrens, 2023). Additionally, as it is estimated that 30% of adults in the US are using smart devices or 'wearables' capable of tracking health data such as nighttime respiration rate, these can increasingly become sources of real-time data for modifying the PBPK/PD model that describes the patient's digital twin, potentially using AI/ML methods. This in turn can lead to timely adjustments in the patient's treatment regimen. However, benefits of access to wearables data must be balanced with control of privacy risks inherent in large scale data collection (Sivakumar, Mone, & Abdumukhtor, 2024).

4. Multiscale modeling of inhaled aerosol transport, deposition, and host-pathogen interactions for predicting health outcomes

Predicting inhaled aerosol transport and deposition via CFPD models is a pivotal aspect of computational aerosol science. Nevertheless, the journey of inhaled chemicals and viruses within the human body extends beyond deposition. Post-deposition, these agents may translocate into the bloodstream, replicate, initiate infections, and elicit immune responses. The extent and impact of these processes are crucial to quantify, rendering the employment of multiscale models imperative to predict health outcomes accurately.

4.1. Significance of multiscale modeling approaches

Modeling the inhalation, deposition, replication, and subsequent immune responses to viruses is a critical challenge. Understanding host cell dynamics (HCD) is essential for advancing therapeutic and preventative measures against viral diseases. Studying the mechanisms of viral infections and the responses of hosts not only helps identify potential therapeutic targets but also deepens our understanding of how the immune system can be leveraged to prevent viral invasions. This knowledge is particularly pertinent in preparing for future pandemics, as understanding the transport, deposition, and immune responses to inhaled pathogens can inform transmission-blocking interventions aimed at pandemic control.

Research methodologies capable of explicitly visualizing and quantifying the interaction between airborne transmission of pathogens like influenza and SARS-CoV-2, pulmonary transport, viral replication, and immune responses, as indicated by variable cell counts over time, remain underdeveloped. Conventional *in vitro* and *in vivo* studies are constrained by operational flexibility and imaging resolution, limiting their ability to address these complex interactions. To bridge this knowledge gap, researchers have been developing multiscale models that integrate CFPD with HCD models (Haghnegahdar et al., 2019b; Hayati et al., 2023a; Li, Kuga, & Ito, 2022, 2023; Li, Kuga, Khoa, & Ito, 2021). The shared workflow for coupling CFPD with HCD is exemplified in Fig. 6, showcasing studies on SARS-CoV-2. Specifically, this modeling framework seeks to simulate and predict.

(1) The emission of exhalation clouds carrying virus-laden droplets,
(2) The rapid evolution of these droplets under varying environmental conditions, such as moisture and temperature,
(3) The inhalation, transport, and deposition within respiratory systems, and
(4) The ensuing host cell dynamics post-deposition in the lungs.

These multiscale models significantly advance the predictive understanding of aerosolized pathogens' behavior and interaction with the human respiratory system. However, further refinements and validations are needed to enhance their predictive power for health outcome endpoints.

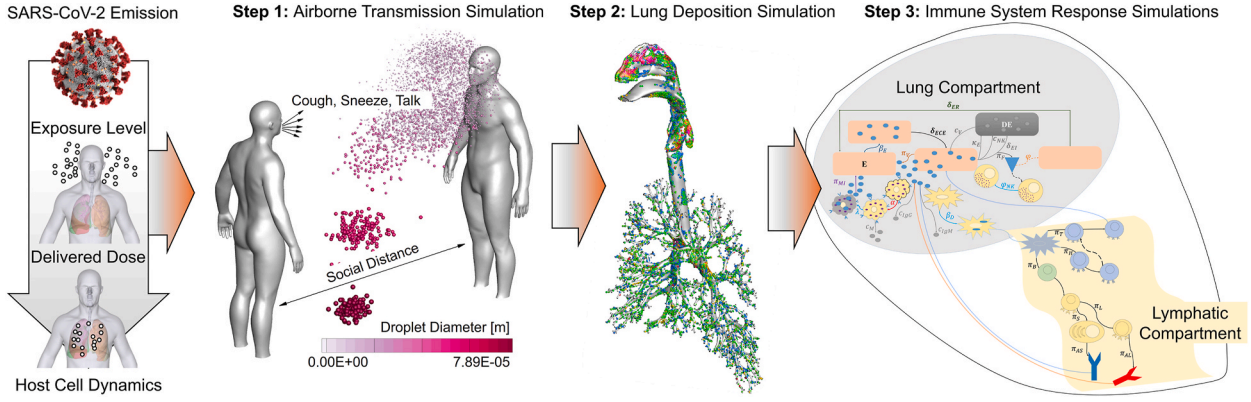

Fig. 6. Schematic representation of the integrated CFPD-HCD modeling approach using SARS-CoV-2 as a case study.

4.2. Existing multiscale CFPD-HCD modeling efforts

Haghnegahdar et al. (Haghnegahdar et al., 2019b) developed a dual-layered CFPD-HCD model to elucidate the transport and fate of inhaled Influenza A Virus (IAV)-laden droplets, as well as the consequent immune responses up to 12 days post-infection. The CFPD model (see **Section 2.3.1**) simulates the transport and deposition of inhaled virus-laden aerosols. Predicted spatial deposition patterns are then used as inputs to the HCD model to determine the regional host dynamic responses. The HCD model consists of a complex system of ODEs that predicts the cell counts or titers of epithelial cells in various states (i.e., uninfected, refectory state, infected), and titers of viruses, mature dendritic cells, helper T cells, cytotoxic T cells, activated B cells, antiviral antibodies, and interferon. The model interlinks simulations at the airway mucosa interface, capturing the initiation of viral replication upon deposition of inhaled particles on epithelial surfaces. Once the virus deposits on the mucosa lining, it binds to the surface of targeted epithelial cells. The deposited aerosol dose is converted to initial viral titer (V_{ini}) as the initial condition for the HCD model. The endocytosis of the virions inside the epithelial cell usually occurs in 1 h after the infection (i.e., post-infection). Subsequently, the innate (IIS) and adaptive immune systems (AIS) are activated. The IIS response consists of released interferons (IFN)-I from the invaded cells and Natural Killers (NK) cells. The AIS response includes a humoral response (antibody-mediated) and cytotoxic lymphocyte agents (Cytotoxic and Helper T cells, B cells) with the activation dependency on Dendritic cells and virus population. Details of the ODEs can be found in (Haghnegahdar et al., 2019b). The authors used these equations to simulate IAV infection dynamics, encompassing viral accumulation and immune reactions in the supraglottic region under varying conditions of oral and nasal inhalation, differentiated by three NaCl concentrations within the IAV-laden droplets. Findings indicate that droplets with elevated NaCl concentrations precipitate increased viral deposition and accelerate immune responses in the supraglottic area. This could exacerbate symptom severity and prolong the recovery period, notably affecting the pharyngeal region.

Li et al. (Li et al., 2022) numerically studied the dynamics of SARS-CoV-2 infection in the mucus layer of the human upper airway. The study combines CFPD and HCD models to simulate the behavior of the virus in the respiratory tract. They use a 3D-shell model to represent the upper respiratory tract with a mucus layer and investigate factors such as diffusion, convection, and the infection rate (β). The findings of this study affirm that the distribution of SARS-CoV-2 in the upper respiratory tract can indeed be affected by factors like diffusion, convection (mucus flow), and the infection rate (β). Notably, the research highlights the pivotal role played by the infection rate β in determining both the time to reach the peak viral load and its duration in the upper respiratory tract. Different values of β were observed to have a profound impact on both the peak viral load and the timing of its occurrence. Furthermore, the numerical experiments underscore the importance of incorporating variables like mucus flow and infection rate when modeling the dynamics of SARS-CoV-2 infection in this context.

Hayati et al. (Hamideh Hayati, Feng, Chen, Kolewe, & Fromen, 2023a) refined the CFPD-HCD model (Haghnegahdar et al., 2019b) to predict SARS-CoV-2 vaccine droplet deposition, transport, and the triggered immune system responses through nasal delivery in a 6-year-old child respiratory system model. The refined HCD model can track an expanded list of 55 cell types, including adaptive immune cells and antibodies, with its accuracy bolstered by clinical data and experimental benchmarks. The study investigated the dynamics of intranasal vaccine droplets targeting the ACE2-receptor-rich olfactory region, aiming to strengthen COVID-19 prevention. The CFPD-HCD model evaluates different nasal spray characteristics, such as cone angles, initial velocities, and droplet compositions, and how they affect vaccine efficacy. The findings reveal that while the initial velocity and droplet composition have minimal impact, the spray cone angle significantly alters vaccine delivery efficiency. The HCD simulation results indicated that the variation in administration strategies did not substantially affect the triggered immune response, a phenomenon attributed to the vaccine droplets' limited coverage of the olfactory region. Consequently, the research emphasizes the necessity of refining the intranasal vaccine formulation and its delivery method to ensure that the vaccine droplets extensively contact the epithelial cells in the olfactory region.

Li et al. (Li, Kuga, & Ito, 2023) studied the dynamics of SARS-CoV-2 within the mucus layer of the human upper airway using a coupled CFPD-HCD model. This approach aims to replicate the impact of mucociliary movement on the transport of viruses within the mucus layer. A 3D-shell model of the upper respiratory tract was constructed from CT data and incorporated the mucus environment by coupling a target cell-limited model with a convection-diffusion term. The novel contributions of this study include a focus on the parameter optimization of the viral dynamics model, dividing the geometric model into multiple compartments, and employing Monolix® (Simulation Plus Inc.) for nonlinear mixed effects (NLME) to assess the influence of various factors like the number of mucus layers.

4.3. Advantages of CFPD-HCD model over traditional HCD simulations

In the context of HCD simulations, integrating CFPD introduces several enhancements. The combined CFPD-HCD model can generate subject-specific and inhalation-profile-specific data on the deposition of inhaled viruses. This leads to more precise initial conditions for subsequent HCD simulations, improving the accuracy of predictions related to cell count changes. This is an improvement over traditional HCD models, which rely on empirical parameters and may not fully capture the detailed viral distribution and dynamics within the respiratory tract. Additionally, the CFPD-HCD model addresses some limitations associated with collecting data from human subjects, particularly in influenza A virus (IAV) studies. The model provides predicted detailed data on virus deposition and replication within the respiratory tract, based on fundamental principles while avoiding the invasiveness of traditional data collection methods.

4.4. Model calibration, validation, and data requirements

The complexity of the ordinary differential equation systems employed in the HCD model introduces numerous unknown coefficients/parameters that require precise calibration using experimental data. It is worth noting that many coefficients/parameters in the HCD model are not theoretically calculable or exhibit significant variations in values. The prevailing strategy for calibrating and validating the HCD model involves comparing viral load or cell count time profiles with data from animal or clinical studies. Therefore, multivariable optimization is typically necessary to find the optimal parameter values for the HCD model. Three steps should be followed for multivariable optimization, as listed below.

- Step 1: Determine biologically reasonable ranges of parameter values from open literature sources (A. Haghnegahdar et al., 2019b; Hayati et al., 2023a).
- Step 2: Utilize a portion of the benchmark experimental data to holistically calibrate the coefficients and parameters using available multivariable optimization techniques, such as controlled elitist genetic algorithms (H. Hayati et al., 2023a).
- Step 3: Employ the remaining benchmark experimental data to validate the HCD model predictions regarding the time profiles of cell count/titer with the coefficient/parameter values optimized in Step 2.

Steps 2 and 3 can be iteratively performed to achieve the best calibration of the coefficient/parameter values. It is essential to emphasize the need for additional clinical data to validate and further improve the models, alongside the importance of employing multivariable optimization methodologies to determine parameter values, as these factors significantly impact the accuracy of HCD modeling.

5. Conclusions

The practical goal of airway deposition modeling of medicinal or toxic environmental particles is to effectively and accurately participate in a process that safeguards or improves public health. Traditionally, this process has involved using empirical models of particle inhalation by healthy subjects and then passing the results of empirical formulae to pharmacodynamic or toxicodynamic empirical models to arrive at predictions of the effectiveness of drugs or the danger posed by toxic particles or vapors. Now with the advent of larger computing power and the availability of non-proprietary databases that provide PBPK/PD models of the fate of particles, it is possible to make more precise, subject-specific predictions. The predictive power and hence usefulness of the whole process depends on (1) the accuracy of the aerosol inhalation modeling, (2) the speed at which accurate modeling can be done, and (3) the accuracy of the pharmacodynamic models that use the data provided by the inhalation modeling. In all three cases, it is anticipated that AI/ML will provide the necessary improvements to make subject-specific prediction useful and widely available. Firstly, AI/ML can be used to learn how subject-specific geometries imaged via CT scan can affect particle deposition, given repeated training by multi-scale 3D/1D models. Second, although the training process for AI is expensive, the trained AI network can then effectively give the best estimate for the deposition of particles in virtually zero time. Thirdly, the increasing amount of data for pharmacodynamic models will allow the necessary training of AI models. With increasing computing power devoted to AI worldwide, the incorporation of new emerging data into existing AI models can be done on a moderate timescale of days or weeks. Thus, it will become feasible to devise ‘digital twins’ for individual patients that best model pharmaceutical interventions and can evolve in parallel with the patient as the models are updated with real-time or regular testing information obtained as the individual responds to treatment. We anticipate the net result of this will be improved predictions and hence improved patient outcomes.

CRediT authorship contribution statement

A.P. Kuprat: Writing – review & editing, Writing – original draft, Conceptualization. **Y. Feng:** Writing – review & editing, Writing – original draft, Funding acquisition, Conceptualization. **R.A. Corley:** Writing – review & editing, Writing – original draft, Conceptualization. **C. Darquenne:** Writing – review & editing, Writing – original draft, Funding acquisition, Conceptualization.

Declaration of competing interest

The authors declare that they have no known competing financial interests or personal relationships that could have appeared to influence the work reported in this paper.

Data availability

No data was used for the research described in the article.

Acknowledgments

This paper was funded by the National Institutes of Health (U01ES028669 from the NIEHS), the National Science Foundation (TI-2234619) and Oklahoma State University CEAT Engineering Research and Seed Funding Program.

References

Andersen, I. K., Sidaros, K., Gesmara, H., Rostrup, E., & Larsson, H. B. (2000). A model system for perfusion quantification using FAIR. *Magnetic Resonance in Imaging, 18*(5), 565–574. https://doi.org/10.1016/s0730-725x(00)00136-3.

Andersen, M. E., & Sarangapani, R. (2001). Physiologically based clearance/extraction models for compounds metabolized in the nose: An example with methyl methacrylate. *Inhalation Toxicology, 13*(5), 397–414. https://doi.org/10.1080/08958370151126284.

Anjilvel, S., & Asgharian, B. (1995). A multiple-path model of particle deposition in the rat lung. *Fundam.Appl.Toxicol., 28*, 41–50.

ANSYS, I. (2024a). *ANSYS fluent theory guide*. Release 2024 R1, Section 12.2.2.1. Stochastic Tracking.

ANSYS, I. (2024b). *ANSYS fluent user's guide*. Release 2024.R1.

Asgharian, B., & Anjilvel, S. (1994). A Monte Carlo calculation of the deposition efficiency of inhaled particles in lower airways. *Journal of Aerosol Science, 25*(4), 711–721.

Asgharian, B., Hofmann, W., & Bergman, R. (2001). Particle deposition in a multiple-path model of the human lung. *Aerosol Science and Technology, 34*(4), 332–339.

Asgharian, B., Price, O., Borojeni, A. A. T., Kuprat, A. P., Colby, S., Singh, R. K., … Darquenne, C. (2022). Influence of alveolar mixing and multiple breaths of aerosol intake on particle deposition in the human lungs. *Journal of Aerosol Science, 166*, Article 106050. https://doi.org/10.1016/j.jaerosci.2022.106050

Bäckman, P., Arora, S., Couet, W., Forbes, B., de Kruijf, W., & Paudel, A. (2018). Advances in experimental and mechanistic computational models to understand pulmonary exposure to inhaled drugs. *European Journal of Pharmaceutical Sciences, 113*, 41–52. https://doi.org/10.1016/j.ejps.2017.10.030

Bass, K., & Worth Longest, P. (2018). Recommendations for simulating microparticle deposition at conditions similar to the upper airways with two-equation turbulence models. *Journal of Aerosol Science, 119*, 31–50. https://doi.org/10.1016/j.jaerosci.2018.02.007

Bauer, C., Krueger, M. A., Lamm, W. J., Glenny, R. W., & Beichel, R. R. (2020). lapdMouse: associating lung anatomy with local particle deposition in mice. *Journal of Applied Physiology, 128*, 309–323.

Beichel, R. R., Glenny, R. W., Bauer, C., Krueger, M. A., & Lamm, W. J. (2019). *Lung anatomy + particle deposition (lapd) mouse archive*. University of Iowa. http://lapdmouse.iibi.uiowa.edu.

Bennett, W. D., & Zeman, K. L. (2005). Effect of race on fine particle deposition for oral and nasal breathing. *Inhalation Toxicology, 17*(12), 641–648. https://doi.org/10.1080/08958370500188984

Bessler, R., & Sznitman, J. (2024). The potential of leveraging electrostatics for improved inhaled drug delivery to the lungs. *Frontiers in Medical Engineering, 1*. https://doi.org/10.3389/fmede.2023.1298251 [Perspective].

Borojeni, A. A. T., Gu, W., Asgharian, B., Price, O., Kuprat, A. P., Singh, R. K., … Darquenne, C. (2023). In silico quantification of intersubject variability on aerosol deposition in the oral airway. *Pharmaceutics, 15*, 160. https://doi.org/10.3390/pharmaceutics15010160

Bush, M. L., Frederick, C. B., Kimbell, J. S., & Ultman, J. S. (1998). A CFD-PBPK hybrid model for simulating gas and vapor uptake in the rat nose. *Toxicology and Applied Pharmacology, 150*(1), 133–145. https://doi.org/10.1006/taap.1998.8407

Chan, T. L., & Lippmann, M. (1980). Experimental measurement and empirical modeling of the regional deposition of inhaled particles in humans. *American Industrial Hygiene Association Journal, 41*, 399–409.

Chen, C., & Zhao, B. (2010). Some questions on dispersion of human exhaled droplets in ventilation room: Answers from numerical investigation. *Indoor Air, 20*(2), 95–111.

Cheng, Y.-S., Zhou, Y., & Chen, B. T. (1999). Particle deposition in a cast of human oral airways. *Aerosol Science and Technology, 31*(4), 286–300. https://doi.org/10.1080/027868299304165

Choi, S., Yoon, S., Jeon, J., Zou, C., Choi, J., Tawhai, M. H., … Lin, C. L. (2019). 1D network simulations for evaluating regional flow and pressure distributions in healthy and asthmatic human lungs. *Journal of Applied Physiology, 127*(1), 122–133. https://doi.org/10.1152/japplphysiol.00016.2019

Christou, S., Chatziathanasiou, T., Angeli, S., Koullapis, P., Stylianou, F., Sznitman, J., & Kassinos, S. C. (2021). Anatomical variability in the upper tracheobronchial tree: Sex-based differences and implications for personalized inhalation therapies. *Journal of Applied Physiology, 130*(3), 678–707. https://doi.org/10.1152/japplphysiol.00144.2020

Clark, K., Vendt, B., Smith, K., Freymann, J., Kirby, J., Koppel, P., … Prior, F. (2013). The cancer imaging archive (TCIA): Maintaining and operating a public information repository. *Journal of Digital Imaging, 26*(6), 1045–1057. https://doi.org/10.1007/s10278-013-9622-7

COPDgene. (2019). *COPDgene*. Retrieved February 8, 2019, from http://www.copdgene.org/.

Corley, R. A., Kabilan, S., Kuprat, A. P., Carson, J. P., Jacob, R. E., Minard, K. R., … Einstein, D. R. (2015). Comparative risks of aldehyde constituents in cigarette smoke using transient computational fluid dynamics/physiologically based pharmacokinetic models of the rat and human respiratory tracts. *Toxicological Sciences, 146*(1), 65–88. https://doi.org/10.1093/toxsci/kfv071

Corley, R. A., Kabilan, S., Kuprat, A. P., Carson, J. P., Minard, K. R., jacob, R. E., … Einstein, D. R. (2012). Comparative computational modeling of airflows and vapor dosimetry in the respiratory tracts of rat, monkey, and human. *Toxicological Sciences, 128*, 500–516.

Corley, R. A., Kuprat, A. P., Suffield, S. R., Kabilan, S., Hinderliter, P. M., Yugulis, K., et al. (2021). New approach methodology for assessing inhalation risks of a contact respiratory cytotoxicant: Computational fluid dynamics-based aerosol dosimetry modeling for cross-species and in vitro comparisons. *Toxicological Sciences, 182*(2), 243–259. https://doi.org/10.1093/toxsci/kfab062

Corley, R. A., Minard, K. R., Kabilan, S., Einstein, D. R., Kuprat, A. P., Harkema, J. R., … Kinzell, J. H. (2009). Magnetic resonance imaging and computational fluid dynamics (CFD) simulations of rabbit nasal airflows for the development of hybrid CFD/PBPK models. *Inhalation Toxicology, 21*(6), 512–518. https://doi.org/10.1080/08958370802598005

Darquenne, C., Corcoran, T. E., Lavorini, F., Sorano, A., & Usmani, O. S. The effects of airway disease on the deposition of inhaled drugs. Expert Opinion on Drug Delivery, 1-16. doi: 10.1080/17425247.2024.2392790.

Darquenne, C., Elliott, A. R., Sibille, B., Smales, E. T., DeYoung, P. D., Theilmann, R. J., et al. (2018). Upper airway dynamic imaging during tidal breathing in awake and asleep subjects with obstructive sleep apnea and healthy controls. *Physiological Reports, 6*, Article e13711. https://doi.org/10.14814/phy2.13711. pp13711–13719.

Darquenne, C., Lamm, W. J., Fine, J. M., Corley, R. A., & Glenny, R. W. (2016). Total and regional deposition of inhaled aerosols in supine healthy subjects and subjects with mild-to-moderate COPD. *Journal of Aerosol Science, 99*, 27–39.

Darquenne, C., & Paiva, M. (1994). One-dimensional simulation of aerosol transport and deposition in the human lung. *Journal of Applied Physiology, 77*, 2889–2898.

Dave, S., Kleinstreuer, C., & Chari, S. (2022). An effective PBPK model predicting dissolved drug transfer from a representative nasal cavity to the blood stream. *Journal of Aerosol Science, 160*, Article 105898.

De Backer, J. W., Vos, W. G., Vinchurkar, S. C., Claes, R., Drollmann, A., Wulfrank, D., … De Backer, W. (2010). Validation of computational fluid dynamics in CT-based airway models with SPECT/CT. *Radiology, 257*(3), 854–862. https://doi.org/10.1148/radiol.10100322

Dominelli, P. B., Ripoll, J. G., Cross, T. J., Baker, S. E., Wiggins, C. C., Welch, B. T., et al. (2018). Sex differences in large conducting airway anatomy. *Journal of Applied Physiology, 125*(3), 960–965. https://doi.org/10.1152/japplphysiol.00440.2018

Einstein, D. R., Neradilak, B., Pollisar, N., Minard, K. R., Wallis, C., Fanucchi, M., … Corley, R. A. (2008). An automated self-similarity analysis of the pulmonary tree of the Sprague-Dawley rat. *The Anatomical Record, 291*(12), 1628–1648. https://doi.org/10.1002/ar.20771

Emmett, P., Aitken, R., & Hannan, W. (1982). Measurements of the total and regional deposition of inhaled particles in the human respiratory tract. *Journal of Aerosol Science, 13*(6), 549–560.

Enlo-Scott, Z., Bäckström, E., Mudway, I., & Forbes, B. (2021). Drug metabolism in the lungs: Opportunities for optimising inhaled medicines. *Expert Opinion on Drug Metabolism and Toxicology, 17*(5), 611–625. https://doi.org/10.1080/17425255.2021.1908262

EPA. (2021). *Multiple-path particle dosimetry (MPPD) model: U.S. EPA technical support documentation and user's guide. (MPPD EPA 2021 v1.01) External Peer Review Draft*. https://assessments.epa.gov/risk/document/&deid=351122.

Feng, Y., Kleinstreuer, C., Castro, N., & Rostami, A. (2016). Computational transport, phase change and deposition analysis of inhaled multicomponent droplet–vapor mixtures in an idealized human upper lung model. *Journal of Aerosol Science, 96*, 96–123.

Feng, Y., Zhao, J., Hayati, H., Sperry, T., & Yi, H. (2021). Tutorial: Understanding the transport, deposition, and translocation of particles in human respiratory systems using Computational Fluid-Particle Dynamics and Physiologically Based Toxicokinetic models. *Journal of Aerosol Science, 151*, Article 105672.
Feng, Y., Zhao, J., Kleinstreuer, C., Wang, Q., Wang, J., Wu, D. H., et al. (2018a). An in silico inter-subject variability study of extra-thoracic morphology effects on inhaled particle transport and deposition. *Journal of Aerosol Science, 123*, 185–207. https://doi.org/10.1016/j.jaerosci.2018.05.010
Fischer, R. P., Volpert, A., Antonino, P., & Ahrens, T. D. (2023). Digital patient twins for personalized therapeutics and pharmaceutical manufacturing. *Front Digit Health, 5*, Article 1302338. https://doi.org/10.3389/fdgth.2023.1302338
Foord, N., Black, A., & Walsh, M. (1978). Regional deposition of 2.5-7.5 μm diameter inhaled particles in healthy male non-smokers. *Journal of Aerosol Science, 9*, 343–357.
Frederick, C. B., Gentry, P. R., Bush, M. L., Lomax, L. G., Black, K. A., Finch, L., … Ultman, J. S. (2001). A hybrid computational fluid dynamics and physiologically based pharmacokinetic model for comparison of predicted tissue concentrations of acrylic acid and other vapors in the rat and human nasal cavities following inhalation exposure. *Inhalation Toxicology, 13*(5), 359–376. https://doi.org/10.1080/08958370117942.
Garcia, G. J., Schroeter, J. D., Segal, R. A., Stanek, J., Foureman, G. L., & Kimbell, J. S. (2009). Dosimetry of nasal uptake of water-soluble and reactive gases: A first study of interhuman variability. *Inhalation Toxicology, 21*(7), 607–618. https://doi.org/10.1080/08958370802320186
Garcia, G. J., Tewksbury, E. W., Wong, B. A., & Kimbell, J. S. (2009). Interindividual variability in nasal filtration as a function of nasal cavity geometry. *Journal of Aerosol Medicine and Pulmonary Drug Delivery, 22*(2), 139–156.
Golshahi, L., Noga, M. L., Vehring, R., & Finlay, W. H. (2013). An in vitro study on the deposition of micrometer-sized particles in the extrathoracic airways of adults during tidal oral breathing. *Annals of Biomedical Engineering, 41*(5), 979–989. https://doi.org/10.1007/s10439-013-0747-0
Grgic, B., Finlay, W. H., Burnell, P. K. P., & Heenan, A. F. (2004). In vitro intersubject and intrasubject deposition measurements in realistic mouth-throat geometries. *Journal of Aerosol Science, 35*, 1025–1040.
Gupta, J. K., Lin, C. H., & Chen, Q. (2011). Transport of expiratory droplets in an aircraft cabin. *Indoor Air, 21*(1), 3–11.
Haefeli-Bleuer, B., & Weibel, E. R. (1988). Morphometry of the human pulmonary acinus. *The Anatomical Record, 220*, 401–414.
Haghnegahdar, A., Feng, Y., Chen, X., & Lin, J. (2018). Computational analysis of deposition and translocation of inhaled nicotine and acrolein in the human body with e-cigarette puffing topographies. *Aerosol Science and Technology, 52*(5), 483–493.
Haghnegahdar, A., Zhao, J., & Feng, Y. (2019). Lung aerosol dynamics of airborne influenza A virus-laden droplets and the resultant immune system responses: An in silico study. *Journal of Aerosol Science, 134*, 34–55. https://doi.org/10.1016/j.jaerosci.2019.04.009
Haghnegahdar, A., Zhao, J., Kozak, M., Williamson, P., & Feng, Y. (2019). Development of a hybrid CFD-PBPK model to predict the transport of xenon gas around a human respiratory system to systemic regions. *Heliyon, 5*(4), Article e01461. https://doi.org/10.1016/j.heliyon.2019.e01461.
Hayati, H., Feng, Y., Chen, X., Kolewe, E., & Fromen, C. (2023). Prediction of transport, deposition, and resultant immune response of nasal spray vaccine droplets using a CFPD-HCD model in a 6-year-old upper airway geometry to potentially prevent COVID-19. *Exp Comput Multiph Flow, 5*(3), 272–289. https://doi.org/10.1007/s42757-022-0145-7
He, C., & Ahmadi, G. (1999). Particle deposition in a nearly developed turbulent duct flow with electrophoresis. *Journal of Aerosol Science, 30*(6), 739–758.
He, Q., Niu, J., Gao, N., Zhu, T., & Wu, J. (2011). CFD study of exhaled droplet transmission between occupants under different ventilation strategies in a typical office room. *Building and Environment, 46*(2), 397–408.
Heyder, J., & Rudolf, G. (1975). Deposition of aerosol particles in the human nose. *Inhaled Particles, 4*(Pt 1), 107–126.
Hofemeier, P., Koshiyama, K., Wada, S., & Sznitman, J. (2018). One (sub-)acinus for all: Fate of inhaled aerosols in heterogeneous pulmonary acinar structures. *European Journal of Pharmaceutical Sciences, 113*, 53–63. https://doi.org/10.1016/j.ejps.2017.09.033
Horsfield, K., Dart, G., Olson, D. E., Filley, G. F., & Cumming, G. (1971). Models of the human bronchial tree. *Journal of Applied Physiology, 31*, 207–217.
Hounam, R. F., Black, A., & Walsh, M. (1970). The deposition of aerosol particles in the nasopharyngeal region of the human respiratory tract. *Inhaled Particles, 1*, 71–80.
ICRP. (1994). Human respiratory tract model for radiological protection. Publication 66. *Annals of the ICRP, 24*(1–3).
ICRP. (2015). Occupational intakes of radionuclides: Part 1. ICRP publication 130. *Annals of the ICRP, 44*(2).
Ismail, M., Comerford, A., & Wall, W. A. (2013). Coupled and reduced dimensional modeling of respiratory mechanics during spontaneous breathing. *Int J Numer Method Biomed Eng, 29*(11), 1285–1305. https://doi.org/10.1002/cnm.2577
Ismail, M., Gravemeier, V., Comerford, A., & Wall, W. A. (2014). A stable approach for coupling multidimensional cardiovascular and pulmonary networks based on a novel pressure-flow rate or pressure-only Neumann boundary condition formulation. *Int J Numer Method Biomed Eng, 30*(4), 447–469. https://doi.org/10.1002/cnm.2611
Kannan, R., Chen, Z., Przekwas, A., Segars, P., Martin, F., Kuczaj, A. K., et al. (2020). Anthropometry-based generation of personalized and population-specific human airway models. *International Journal for Numerical Methods in Biomedical Engineering, 36*(5), Article e3324. https://doi.org/10.1002/cnm.3324
Kannan, R., Singh, N., & Przekwas, A. (2018). A compartment–quasi-3D multiscale approach for drug absorption, transport, and retention in the human lungs. *International journal for numerical methods in biomedical engineering, 34*(5), Article e2955.
Khajeh-Hosseini-Dalasm, N., & Longest, P. W. (2015). Deposition of particles in the alveolar airways: Inhalation and breath-hold with pharmaceutical aerosols. *Journal of Aerosol Science, 79*, 15–30. https://doi.org/10.1016/j.jaerosci.2014.09.003
Kimbell, J. S., & Subramaniam, R. P. (2001). Use of computational fluid dynamics models for dosimetry of inhaled gases in the nasal passages. *Inhalation Toxicology, 13*(5), 325–334. https://doi.org/10.1080/08958370120442.
Kleinstreuer, C., & Feng, Y. (2013). Computational analysis of non-spherical particle transport and deposition in shear flow with application to lung aerosol dynamics–a review. *Journal of Biomechanical Engineering, 135*(2), Article 021008. https://doi.org/10.1115/1.4023236
Kolanjiyil, A., & Kleinstreuer, C. (2017). Computational analysis of aerosol-dynamics in a human whole-lung airway model. *Journal of Aerosol Science, 114*, 301–316. https://doi.org/10.1016/j.jaerosci.2017.10.001.
Koshiyama, K., & Wada, S. (2015). Mathematical model of a heterogeneous pulmonary acinus structure. *Computers in Biology and Medicine, 62*, 25–32. https://doi.org/10.1016/j.compbiomed.2015.03.032
Koullapis, P. G., Hofemeier, P., Sznitman, J., & Kassinos, S. C. (2018). An efficient computational fluid-particle dynamics method to predict deposition in a simplified approximation of the deep lung. *European Journal of Pharmaceutical Sciences, 113*, 132–144. https://doi.org/10.1016/j.ejps.2017.09.016
Koullapis, P. G., Kassinos, S. C., Bivolarova, M. P., & Melikov, A. K. (2016). Particle deposition in a realistic geometry of the human conducting airways: Effects of inlet velocity profile, inhalation flowrate and electrostatic charge. *Journal of Biomechanics, 49*(11), 2201–2212. https://doi.org/10.1016/j.jbiomech.2015.11.029
Koullapis, P., Ollson, B., Kassinos, S. C., & Sznitman, J. (2019). Multiscale in silico lung modeling strategies for aerosol inhalation therapy and drug delivery. *Curr Opin Biomed Eng, 11*, 130–136. https://doi.org/10.1016/j.cobme.2019.11.003
Koullapis, P. G., Stylianou, F. S., Sznitman, J., Olsson, B., & Kassinos, S. C. (2020). Towards whole-lung simulations of aerosol deposition: A model of the deep lung. *Journal of Aerosol Science, 144*, Article 105541. https://doi.org/10.1016/j.jaerosci.2020.105541
Kuerten, J. G. M. (2016). Point-particle DNS and LES of particle-laden turbulent flow-a state-of-the-art review. Flow. *Turbulence and Combustion, 97*, 689–713. https://doi.org/10.1007/s10494-016-9765-y.
Kuga, K., & Ito, K. (2019). Comparative inhalation exposure/toxicology analysis of e-cigarette vapors with different puffing behaviors using PBPK-CSP-CFD approach. *IOP Conf. Ser.: Mater. Sci. Eng., 609*, 042004 https://doi.org/10.1088/1757-899X/609/4/042004.
Kuga, K., Ito, K., Chen, W., Wang, P., & Kumagai, K. (2020). A numerical investigation of the potential effects of e-cigarette smoking on local tissue dosimetry and the deterioration of indoor air quality. *Indoor Air, 30*(5), 1018–1038.
Kuprat, A. P., Jalali, M., Jan, T., Corley, R. A., Asgharian, B., Price, O., … Darquenne, C. (2021). Efficient bi-directional coupling of 3D computational fluid-particle dynamics and 1D Multiple Path Particle Dosimetry lung models for multiscale modeling of aerosol dosimetry. *Journal of Aerosol Science, 151*, Article 105647.
Kuprat, A. P., Kabilan, S., Carson, J. P., Corley, R. A., & Einstein, D. R. (2013). A bidirectional coupling procedure applied to multiscale respiratory modeling. *Journal of Computational Physics, 244*. https://doi.org/10.1016/j.jcp.2012.10.021

Kuprat, A. P., Price, O., Asgharian, B., Singh, R. K., Colby, S., Yugulis, K., … Darquenne, C. (2023). Automated bidirectional coupling of multiscale models of aerosol dosimetry: Validation with subject-specific deposition data. *Journal of Aerosol Science, 174*, Article 106233. https://doi.org/10.1016/j.jaerosci.2023.106233

Kwon, Y. (2001). *Handbook of essential pharmacokinetics, pharmacodynamics and drug metabolism for industrial scientists*. Springer Science & Business Media.

Ladumor, M. K., & Unadkat, J. D. (2022). Predicting regional respiratory tissue and systemic concentrations of orally inhaled drugs through a novel PBPK model. *Drug Metabolism and Disposition, 50*(5), 519–528.

Li, A., & Ahmadi, G. (1992). Dispersion and deposition of spherical particles from point sources in a turbulent channel flow. *Aerosol Science and Technology, 16*(4), 209–226.

Li, H., Kuga, K., & Ito, K. (2022). SARS-CoV-2 dynamics in the mucus layer of the human upper respiratory tract based on host–cell dynamics. *Sustainability, 14*(7), 3896.

Li, H., Kuga, K., & Ito, K. (2023). Visual prediction and parameter optimization of viral dynamics in the mucus milieu of the upper airway based on CFPD-HCD analysis. *Computer Methods and Programs in Biomedicine, 238*, Article 107622.

Li, H., Kuga, K., Khoa, N. D., & Ito, K. (2021). *Effects of initial conditions and parameters on the prediction of SARS-CoV-2 viral load in the upper respiratory tract based on host-cell dynamics*.

Li, X., Shang, Y., Yan, Y., Yang, L., & Tu, J. (2018). Modelling of evaporation of cough droplets in inhomogeneous humidity fields using the multi-component Eulerian-Lagrangian approach. *Building and Environment, 128*, 68–76.

Lippmann, M. (1976). Regional Deposition of Particles in the Human Respiratory Tract. In R. Terjung (Ed.), *Comprehensive Physiology*, 2011 https://doi.org/10.1002/cphy.cp090114.

Longest, P. W., Bass, K., Dutta, R., Rani, V., Thomas, M. L., El-Achwah, A., et al. (2019). Use of computational fluid dynamics deposition modeling in respiratory drug delivery. *Expert Opinion on Drug Delivery, 16*(1), 7–26. https://doi.org/10.1080/17425247.2019.1551875

Longest, P. W., & Hindle, M. (2011). Numerical model to characterize the size increase of combination drug and hygroscopic excipient nanoparticle aerosols. *Aerosol Science and Technology, 45*(7), 884–899. https://doi.org/10.1080/02786826.2011.566592

Longest, P. W., & Holbrook, L. T. (2012). In silico models of aerosol delivery to the respiratory tract—development and applications. *Advanced Drug Delivery Reviews, 64*, 296–311.

Longest, P. W., & Xi, J. (2007). Effectiveness of direct Lagrangian tracking models for simulating nanoparticle deposition in the upper airways. *Aerosol Science and Technology, 41*(4), 380–397.

Menter, F. R. (1993). Zonal two equation k-w models for aerodynamic flows. July 6–9. In *Paper presented at the 23rd fluid dynamics, plasmadynamics, and lasers conference, July 6-9 1993, Orlando, FL, USA* https://doi.org/10.2514/6.1993-2906.

Menter, F. R. (1994). Two-equation eddy-viscosity turbulence models for engineering applications. *AIAA Journal, 32*(8), 1598–1605. https://doi.org/10.2514/3.12149

Menter, F. R., Kuntz, M., & Langtry, R. (2003). Ten years of industrial experience with the SST turbulence model. In *Proceedings of the 4th International Symposium on Turbulence, heat and mass transfer* (pp. 625–632). Antalya, Turkey, 12-17 October, 2003.

Mofakham, A. A., & Ahmadi, G. (2020). On random walk models for simulation of particle-laden turbulent flows. *International Journal of Multiphase Flow, 122*, Article 103157. https://doi.org/10.1016/j.ijmultiphaseflow.2019.103157

Moghadam, M. E., Vignon-Clementel, I. E., Figliola, R., & Marsden, A. L. (2013). A modular numerical method for implicit 0D/3D coupling in cardiovascular finite element simulations. *Journal of Computational Physics, 244*, 63–79. https://doi.org/10.1016/j.jcp.2012.07.035

Morris, J. B., & Hubbs, A. F. (2009). Inhalation dosimetry of diacetyl and butyric acid, two components of butter flavoring vapors. *Toxicological Sciences, 108*(1), 173–183. https://doi.org/10.1093/toxsci/kfn222

NBIA. (2019). National biomedical imaging archive (NBIA). Retrieved 02/08/2019, from https://github.com/CBIIT/NBIA-TCIA.

1997 NCRP. (1997). *Deposition, retention, and dosimetry of inhaled radioactive substances. NCRP Report No. 125. Bethesda, MD: NCRP*. https://ncrponline.org/shop/reports/report-no-125-deposition-retention-and-dosimetry-of-inhaled-radioactive-substances-1997/.

Nikander, K., von Hollen, D., & Larhrib, H. (2017). The size and behavior of the human upper airway during inhalation of aerosols. *Expert Opinion on Drug Delivery, 14*(5), 621–630. https://doi.org/10.1080/17425247.2016.1227780

Oakes, J. M. (2024). The utility of hybrid in silico models of airflow and aerosol dosimetry in the lung. *Journal of Biomechanics, 168*, Article 112126. https://doi.org/10.1016/j.jbiomech.2024.112126

Oakes, J. M., Marsden, A., Grandmont, C., Shadden, S. C., Darquenne, C., & Vignon-Clementel, I. E. (2014). Airflow and particle deposition simulations in health and emphysema: From in-vivo to in-silico animal experiments. *Annals of Biomedical Engineering, 42*, 899–914.

Oakes, J. M., Shadden, S. C., Grandmont, C., & Vignon-Clementel, I. E. (2017). Aerosol transport throughout inspiration and expiration in the pulmonary airways. *Int J Numer Method Biomed Eng, 33*(9). https://doi.org/10.1002/cnm.2847

Oesch, F., Fabian, E., & Landsiedel, R. (2019). Xenobiotica-metabolizing enzymes in the lung of experimental animals, man and in human lung models. *Arch Toxicol, 93*(12), 3419–3489. https://doi.org/10.1007/s00204-019-02602-7

Palazzolo, D. L., Nelson, J. M., Ely, E. A., Crow, A. P., Distin, J., & Kunigelis, S. C. (2017). The effects of electronic cigarette (ECIG)-Generated aerosol and conventional cigarette smoke on the mucociliary transport velocity (MTV) using the bullfrog (R. Catesbiana) palate paradigm. *Frontiers in Physiology, 8*, 1023. https://doi.org/10.3389/fphys.2017.01023

Peiró, J., & Veneziani, A. (2009). Reduced models of the cardiovascular system. In Formaggia, L., Quarteroni, A., & Veneziani, A. (Eds.), Cardiovascular Mathematics: Modeling and simulation of the circulatory system (pp. 347–394). Springer-Verlag (Milano). https://doi.org/10.1007/978-88-470-1152-6_10.

Poorbahrami, K., Mummy, D. G., Fain, S. B., & Oakes, J. M. (2019). Patient-specific modeling of aerosol delivery in healthy and asthmatic adults. *Journal of Applied Physiology, 127*(6), 1720–1732. https://doi.org/10.1152/japplphysiol.00221.2019

Rahman, M. M., Zhao, M., Islam, M. S., Dong, K., & Saha, S. C. (2022). Nanoparticle transport and deposition in a heterogeneous human lung airway tree: An efficient one path model for CFD simulations. *European Journal of Pharmaceutical Sciences, 177*, Article 106279. https://doi.org/10.1016/j.ejps.2022.106279

Rasmussen, T., Swift, D., Hilberg, O., & Pedersen, O. (1990). Influence of nasal passage geometry on aerosol particle deposition in the nose. *Journal of Aerosol Medicine, 3*(1), 15–25.

Rostami, A. A. (2009). Computational modeling of aerosol deposition in respiratory tract: A review. *Inhalation Toxicology, 21*, 262–290.

Rostami-Hodjegan, A. (2018). Reverse translation in PBPK and QSP: Going backwards in order to go forward with confidence. *Clinical Pharmacology & Therapeutics, 103*(2), 224–232. https://doi.org/10.1002/cpt.904

Sadafi, H., Monshi Tousi, N., De Backer, W., & De Backer, J. (2024). Validation of computational fluid dynamics models for airway deposition with SPECT data of the same population. *Scientific Reports, 14*(1), 5492. https://doi.org/10.1038/s41598-024-56033-1

Salim, S., Ong, K., & Cheah, S. (2011). Comparison of RANS, URANS and LES in the prediction of airflow and pollutant dispersion. In *Proceedings of the World Congress on Engineering and Computer Science 2011 Vol II WCECS 2011, October 19–21, 2011, San Francisco, USA*. https://www.iaeng.org/publication/WCECS2011/WCECS2011_pp673-678.pdf.

Schroeter, J. D., Kimbell, J. S., Andersen, M. E., & Dorman, D. C. (2006). Use of a pharmacokinetic-driven computational fluid dynamics model to predict nasal extraction of hydrogen sulfide in rats and humans. *Toxicological Sciences, 94*(2), 359–367. https://doi.org/10.1093/toxsci/kfl112

Schroeter, J. D., Kimbell, J. S., Asgharian, B., Tewksbury, E. W., Sochaski, M., Foster, M. L., … Andersen, M. E. (2013). Inhalation dosimetry of hexamethylene diisocyanate vapor in the rat and human respiratory tracts. *Inhalation Toxicology, 25*(3), 168–177. https://doi.org/10.3109/08958378.2013.768314

Schroeter, J. D., Kimbell, J. S., Bonner, A. M., Roberts, K. C., Andersen, M. E., & Dorman, D. C. (2006). Incorporation of tissue reaction kinetics in a computational fluid dynamics model for nasal extraction of inhaled hydrogen sulfide in rats. *Toxicological Sciences, 90*(1), 198–207. https://doi.org/10.1093/toxsci/kfj072

Schroeter, J. D., Kimbell, J. S., Gross, E. A., Willson, G. A., Dorman, D. C., Tan, Y. M., et al. (2008). Application of physiological computational fluid dynamics models to predict interspecies nasal dosimetry of inhaled acrolein. *Inhalation Toxicology, 20*(3), 227–243. https://doi.org/10.1080/08958370701864235.

Schwab, R. J., Gefter, W. B., Hoffman, E. A., Gupta, K. B., & Pack, A. I. (1993). Dynamic upper airway imaging during awake respiration in normal subjects and patients with sleep disordered breathing. *American Review of Respiratory Disease, 148*, 1385–1400.

Siemens Digital IndustriesSoftware. (2022). *Simcenter STAR-CCM+ user guid*. Release 2206 https://plm.sw.siemens.com/en-US/simcenter/fluids-thermal-simulation/star-ccm/.

Sivakumar, C. L. V., Mone, V., & Abdumukhtor, R. (2024). Addressing privacy concerns with wearable health monitoring technology. *WIREs Data Mining and Knowledge Discovery, 14*(3), Article e1535. https://doi.org/10.1002/widm.1535

Sperry, T., Feng, Y., Song, C., & Shi, Z. (2024). CFPD-PK simulation of inhaled Delta-9-tetrahydrocannabinol aerosol dynamics: Transport, deposition, and translocation in a mouth-to-G10 subject-specific human airway. *Journal of Aerosol Science*, Article 106334.

Stahlhofen, W., Gebhart, J., & Heyder, J. (1980). Experimental determination of the regional deposition of aerosol particles in the human respiratory tract. *American Industrial Hygiene Association Journal, 41*, 385–398.

Stahlhofen, W., Gebhart, J., & Heyder, J. (1981). Biological variability of regional deposition of aerosol particles in the human respiratory tract. *American Industrial Hygiene Association Journal, 42*(5), 348–352.

Stahlhofen, W., Gebhart, J., Heyder, J., & Scheuch, G. (1983). New regional deposition data of the human respiratory tract. *Journal of Aerosol Science, 14*(3), 186–188.

Sweeney, L. M., Andersen, M. E., & Gargas, M. L. (2004). Ethyl acrylate risk assessment with a hybrid computational fluid dynamics and physiologically based nasal dosimetry model. *Toxicological Sciences, 79*(2), 394–403. https://doi.org/10.1093/toxsci/kfh116

Taulbee, D. B., & Yu, C. P. (1975). A theory of aerosol deposition in human respiratory tract. *Journal of Applied Physiology, 38*, 77–85.

Tawhai, M. H., Hunter, P., Tschirren, J., Reinhardt, J., McLennan, G., & Hoffman, E. A. (2004). CT-based geometry analysis and finite element models of the human and ovine bronchial tree. *Journal of Applied Physiology, 97*, 2310–2321.

Tawhai, M. H., Pullan, A. J., & Hunter, P. J. (2000). Generation of an anatomically based three-dimensional model of the conducting airways. *Annals of Biomedical Engineering, 28*, 793–802. https://doi.org/10.1114/1.1289457.

Tian, G., Longest, P. W., Su, G., Walenga, R. L., & Hindle, M. (2011). Development of a stochastic individual path (SIP) model for predicting the tracheobronchial deposition of pharmaceutical aerosols: Effects of transient inhalation and sampling the airways. *Journal of Aerosol Science, 42*(11), 781–799. https://doi.org/10.1016/j.jaerosci.2011.07.005.

Tian, L., & Ahmadi, G. (2007). Particle deposition in turbulent duct flows—comparisons of different model predictions. *Journal of Aerosol Science, 38*(4), 377–397. https://doi.org/10.1016/j.jaerosci.2006.12.003

Vinchurkar, S., De Backer, L., Vos, W., Van Holsbeke, C., De Backer, J., & De Backer, W. (2012). A case series on lung deposition analysis of inhaled medication using functional imaging based computational fluid dynamics in asthmatic patients: Effect of upper airway morphology and comparison with in-vivo data. *Inhalation Toxicology, 24*, 81–88.

Vulović, A., Šušteršič, T., Cvijić, S., Ibrić, S., & Filipović, N. (2018). Coupled in silico platform: Computational fluid dynamics (CFD) and physiologically-based pharmacokinetic (PBPK) modelling. *European Journal of Pharmaceutical Sciences, 113*, 171–184.

Walenga, R. L., & Longest, P. W. (2016). Current inhalers deliver very small doses to the lower tracheobronchial airways: Assessment of healthy and constricted lungs. *Journal of Pharmaceutical Sciences, 105*(1), 147–159. https://doi.org/10.1016/j.xphs.2015.11.027

Weibel, E. R. (1963). *Morphometry of the human lung*. New York: Academic Press.. https://doi.org/10.1007/978-3-642-87553-3

Yamada, Y., Yamada, M., Chubachi, S., Yokoyama, Y., Matsuoka, S., Tanabe, A., … Jinzaki, M. (2020). Comparison of inspiratory and expiratory lung and lobe volumes among supine, standing, and sitting positions using conventional and upright CT. *Scientific Reports, 10*(1), Article 16203. https://doi.org/10.1038/s41598-020-73240-8

Yang, Y. K., Kang, I. S., Hwang, J. H., & Park, J. C. (2017). CFD simulation for air-borne infection analysis in AII-room. *International Journal of Mechanical & Mechatronics Engineering, 11*(5), 1047–1052. https://doi.org/10.5281/zenodo.1130426.

Yeh, H. C., & Schum, G. M. (1980). Models of human lung airways and their application to inhaled particle deposition. *Bulletin of Mathematical Biology, 42*, 461–480.

Yoo, S.-J., & Ito, K. (2018a). Assessment of transient inhalation exposure using in silico human model integrated with PBPK-CFD hybrid analysis. *Sustainable Cities and Society, 40*, 317–325.

Yoo, S.-J., & Ito, K. (2018b). Numerical prediction of tissue dosimetry in respiratory tract using computer simulated person integrated with physiologically based pharmacokinetic–computational fluid dynamics hybrid analysis. *Indoor and Built Environment, 27*(7), 877–889.

Zhang, Z., & Kleinstreuer, C. (2011). Laminar-to-turbulent fluid–nanoparticle dynamics simulations: Model comparisons and nanoparticle-deposition applications. *International Journal for Numerical Methods in Biomedical Engineering, 27*(12), 1930–1950. https://doi.org/10.1002/cnm.1447

Zhang, L., & Li, Y. (2012). Dispersion of coughed droplets in a fully-occupied high-speed rail cabin. *Building and Environment, 47*, 58–66. https://doi.org/10.1016/j.buildenv.2011.03.015

Zhang, X., Li, F., Rajaraman, P. K., Choi, J., Comellas, A. P., Hoffman, E. A., … Lin, C. L. (2022). A computed tomography imaging-based subject-specific whole-lung deposition model. *European Journal of Pharmaceutical Sciences, 177*, Article 106272. https://doi.org/10.1016/j.ejps.2022.106272

Zhao, J., Feng, Y., Bezerra, M., Wang, J., & Sperry, T. (2019). Numerical simulation of welding fume lung dosimetry. *Journal of Aerosol Science*. https://doi.org/10.1016/j.jaerosci.2019.05.006

Zhao, J., Feng, Y., Tian, G., Taylor, C., & Arden, N. S. (2021). Influences of puff protocols and upper airway anatomy on cannabis pharmacokinetics: A CFPD-PK study. *Computers in Biology and Medicine, 132*, Article 104333.

Zhao, J., Haghnegahdar, A., Feng, Y., Patil, A., Kulkarni, N., Singh, G. J. P., … Bharadwaj, R. (2022). Prediction of the carrier shape effect on particle transport, interaction and deposition in two dry powder inhalers and a mouth-to-G13 human respiratory system: A CFD-DEM study. *Journal of Aerosol Science, 160*, Article 105899.

Zhu, S., Kato, S., & Yang, J.-H. (2006). Study on transport characteristics of saliva droplets produced by coughing in a calm indoor environment. *Building and Environment, 41*(12), 1691–1702. https://doi.org/10.1016/j.buildenv.2005.06.024